JOTCS A
Journal of the Turkish Chemical Society
Section: A
Chemistry
TURKISH CHEMICAL SOCIETY

Synthesis of Novel Oxadiazole Derivatives, Molecular Properties Prediction, and Molecular Docking Studies

Zühal KILIC-KURT*

Ankara University, Faculty of Pharmacy, Department of Pharmaceutical Chemistry, Tandogan, Ankara, Turkey

Abstract: In this work, the synthesis of novel 1,3,4-oxadiazole derivatives was reported. A good molecular properties profile was predicted for the target compounds. In drug-likeness prediction, compound **4b** and **8b** possess the highest score of 0.31 and 0.33, respectively. Since the compounds have good bioactivity scores as a kinase inhibitor, possible interactions of compounds with VEGFR-2 kinase and probable binding conformations were evaluated by molecular docking. All compounds formed hydrogen bonding interactions with Asp1046 amino acid of key residues.

Keywords: Oxadiazole, VEGFR-2, docking.

Submitted: March 18, 2020. **Accepted:** July 16, 2020.

Cite this: KILIC-KURT Z. Synthesis of Novel Oxadiazole Derivatives, Molecular Properties Prediction, and Molecular Docking Studies. JOTCSA. 2020; 7(3): 753-74.

DOI: https://doi.org/10.18596/jotcsa.705951.

***Corresponding author.** E-mail: zkurt@ankara.edu.tr.

INTRODUCTION

The 1,3,4-oxadiazole ring is often used in drug design research due to its effect on the ADME properties of the compounds. It has a better metabolic and solubility profile. Oxadiazole ring can interact with ligand via its hydrogen bond acceptor properties. It has been used instead of ester and amide functional groups for bioisosteric replacements. Moreover, to provide an appropriate orientation of the molecule, an oxadiazole ring can be used as a flat aromatic linker (1-2). To date, several compounds based on oxadiazole moiety have been reported with different pharmacological activities such as antibacterial, antifungal, antiviral, antitubercular (3), anticancer (4) as well as other biological activities. 1,3,4-Oxadiazole-based compounds such as **Zibotentan** (ZD4054) and **Ataluren** (Figure 1) are in the late-stage clinical trial for prostate cancer and cystic fibrosis, respectively (5-6). Moreover, several oxadiazole derivatives were reported to have potential anticancer activity through a different mechanism (7-9). Compound **I** (Figure 1) exhibited significant inhibition on tubulin polymerization and caused mitotic arrest in A431 human epidermoid cells (10). Compound **II** (Figure 1) displayed the inhibitory effect on the proliferation of SMMC-7721 cell line (11). 1,3,4-Oxadiazole based compound **III** (Figure 1) combined with alanine amino acid was found as a selective inhibitor of histone deacetylase-8 (HDAC-8) and showed inhibition on proliferation of breast cancer cell lines (12). Another 1,3,4-oxadiazole based compound **IV** (Figure 1) inhibited NF-κB signaling pathway. It also induced antiproliferative effect and apoptosis in hepatocellular carcinoma (13). Compound **V** (Figure 1) exhibited potent anticancer activity towards MCF-7 cells and significant EGFR tyrosine inhibition (14). Compound **VI** (Figure 1) showed strong inhibitory activity against focal adhesion kinase (FAK) and unusual

antiproliferative activity related to the 5-Fluorouracil (15). Oxadiazole derivative bearing ((pyridin-4-yl)ethyl)pyridine moiety (**VII**) was reported as a selective and competitive inhibitor of VEGFR-2 with IC_{50} value of 31 nM (16). Oxadiazole derivative combined with pyrrolotriazine scaffold (**VIII**) exhibited potent enzymatic (IC_{50} = 11 nM) and VEGF-stimulated HUVEC cellular inhibitory activity against VEGFR-2 (IC_{50} = 11 nM) (17). Another oxadiazole based compound **IX** demonstrated nanomolar inhibitory potency toward VEGFR-2 in both enzymatic and cellular phosphorylation assays. It also showed strong activity in tubulin cellular G2M block assay in the nanomolar range (18).

Based on the above-mentioned findings, in this work, novel 1,3,4-oxadiazole derivatives bearing benzo[*b*]thiophen (**4a-c**) and thiophene (**8a-c**) scaffolds were designed and synthesized. All the synthesized compounds have been subjected to the prediction of molecular properties, bioactivity, and drug-likeness scores. Bioactivity score prediction results suggest that synthesized compounds can be active (**4a-c**; >0) or moderate active (**8a-c**; -0.5-0) against kinases. It is reported that oxadiazole derivatives have strong inhibitor activity on kinases such as EGFR (19-21), FAK (15, 22) and VEGFR-2 (16-18,23,24) proteins. So, to make target prediction for designed compounds, molecular docking studies of compounds in EGFR, FAK, and VEGFR-2 kinases were performed using Autodock Vina, and results were discussed.

MATERIALS AND METHODS

Synthesis of methyl esters (1 and 5)

Carboxylic acids (1 eq) and a catalytic amount of concd. H_2SO_4 (0.1 mL) were refluxed in MeOH (5 mL) overnight. Then, the solvent was evaporated and satd. $NaHCO_3$ (aq) was added. The white precipitate was filtered, then washed with water, and dry to obtain the methyl esters **1** and **5** (25).

Synthesis of carbohydrazide derivatives (2-6)

Methyl esters (**1** and **5**, 1 eq) were dissolved in methanol (15 mL), hydrazine hydrate (10 eq) was added and heated at reflux for 3 hours, cooled and the precipitate filtered to afford hydrazide derivatives **2** and **6** (26).

Synthesis of 2-(benzo[*b*]thiophen-2-yl)-5-(chloromethyl)-1,3,4-oxadiazole (3) and 2-(chloromethyl)-5-(thiophen-2-yl)-1,3,4-oxadiazole (7)

A mixture of chloroacetic acid (1.2 eq) and an appropriate acid hydrazide (1 eq, **2** or **6**) in 7-8 mL of $POCl_3$ was refluxed for 5-6 h. Then, to the mixture, ice was added, and 2 M NaOH solution was added until pH=6-7. The white precipitate was filtered and washed with water. Purification was performed by column chromatography using n-hexane:EtOAc (7:1) mixture to afford pure compounds **3** and **7** in moderate yields.

2-(Benzo[b]thiophen-2-yl)-5-(chloromethyl)-1,3,4-oxadiazole (3)

CAS number:1250681-18-5. Mp: 175 °C. Proton NMR (DMSO-d_6) δ: 5.15 (s, 2H, CH_2), 7.46-7.54 (m, 2H), 8.03 (d, 1H, J=6.8 Hz), 8.11 (d, 1H, J=8.4 Hz), 8.25 (s, 1H). Carbon NMR (DMSO-d_6, 100 MHz) δ: 33.08, 122.89, 123.43, 125.42, 125.46, 127.09, 127.81, 138.72, 140.07, 161.31, 162.85. Mass (ESI) *m/z*: 251.78 [M+H].

2-(Chloromethyl)-5-(thiophen-2-yl)-1,3,4-oxadiazole (7)

Mp: 91 °C. Proton NMR (DMSO-d_6) δ: 5.09 (s, 2H, CH_2), 7.29 (dd, 1H, J= 6.8 Hz, 4 Hz), 7.85 (dd, 1H, J=4 Hz, 1.2 Hz), 7.97 (dd, 1H, J=4 Hz, 1.2 Hz). Carbon NMR (DMSO-d_6, 100 MHz) δ: 33.13, 123.65, 128.90, 130.85, 132.20, 161.27, 162.26. (27).

Synthesis of 2-(benzo[*b*]thiophen-2-yl)-5-((4-substituted-piperazin-1-yl) methyl)-1,3,4-oxadiazole (4a-c) and 2-((4-substituted-piperazin-1-yl)methyl)-5-(thiophen-2-yl)-1,3,4-oxadiazole derivatives (8a-c)

The intermediates **3** or **7** (1 eq), appropriate piperazine (2 eq), potassium carbonate (2 eq) and potassium iodide (1 eq) were refluxed in acetone (30 mL) for 5-6 h. Then, acetone was evaporated to dryness, and water was added. Ethyl acetate extraction was done, and purification was performed by silica gel column chromatography with dichloromethane: methanol or n-hexane: ethyl acetate to give the compounds **4a**-**c** and **8a**-**c** in 40–60% yields.

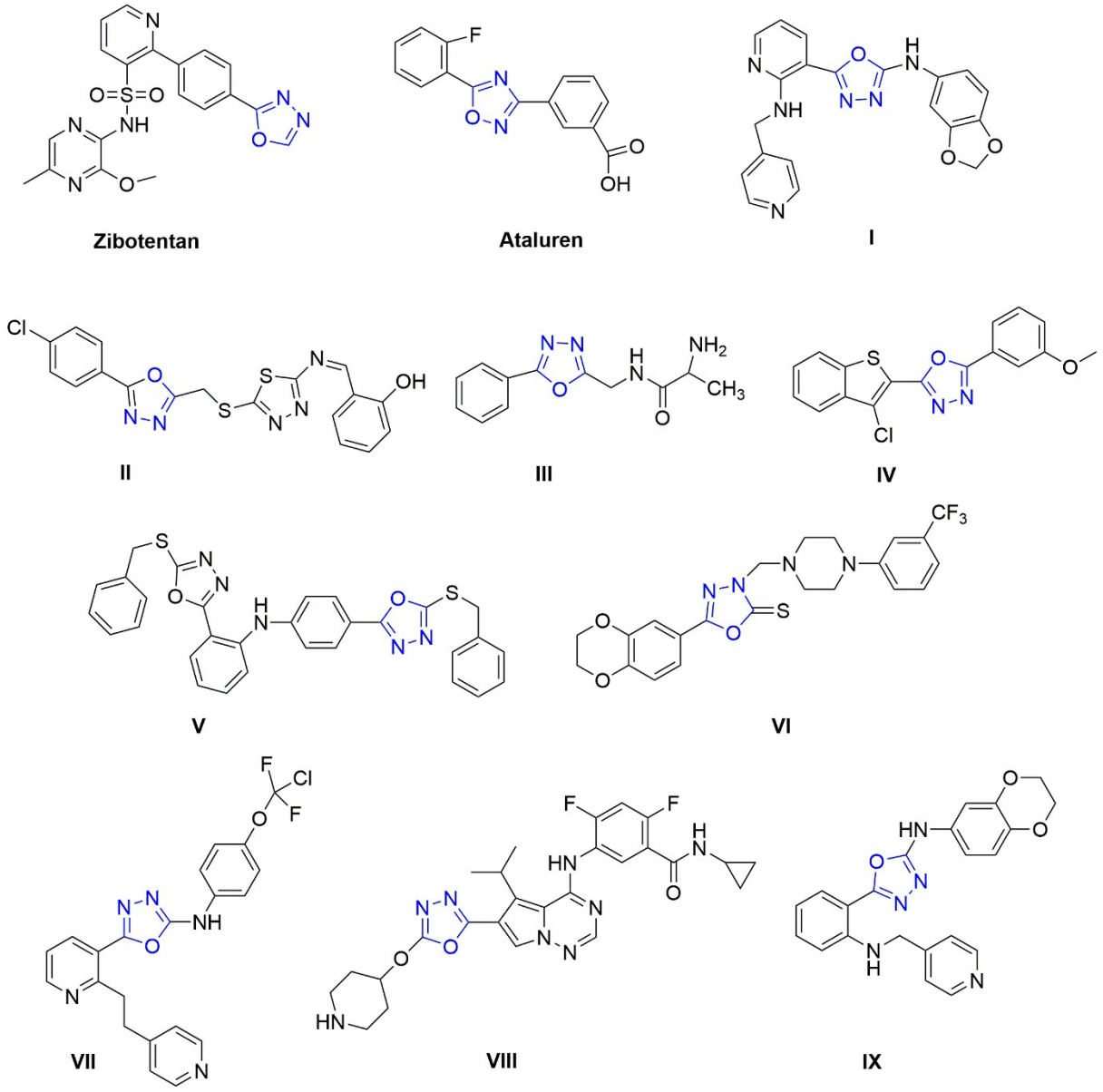

Figure 1. 1,3,4-Oxadiazole compounds having anticancer activity.

2-(Benzo[b]thiophen-2-yl)-5-((4-methylpiperazin-1-yl)methyl)-1,3,4-oxadiazole (4a)

Yield: 45%. Mp: 128 °C. Proton NMR (DMSO-d_6) δ: 2.19 (s, 3H, CH_3), 2.30 (bs, 4H, H-a), 2.51 (bs, 4H, H-b), 3.86 (s, 2H, CH_2), 7.44-7.52 (m, 2H, H-5,6), 8.01 (dd, 1H, J=6.8 Hz, 1.6 Hz, H-4), 8.08 (d, 1H, J=7.6 Hz, H-7), 8.19 (s, 1H, H-3). Carbon NMR (DMSO-d_6, 100 MHz) δ: 45.57 (CH_3), 50.97 (CH_2), 51.97 (piperazine-b), 54.40 (piperazine-a), 122.83, 124.04, 125.26, 125.37, 126.86, 127.18, 138.78, 139.89, 160.76, 163.78. Mass (ESI) *m/z*: 315.55 [M+H].

2-(Benzo[b]thiophen-2-yl)-5-((4-(3-methoxyphenyl)piperazin-1-yl)methyl)-1,3,4-oxadiazole (4b)

Yield: 76%. Mp: 165 °C. Proton NMR (DMSO-d_6) δ: 2.68 (t, 4H, H-b), 3.15 (t, 4H, H-a), 3.69 (s, 3H, OCH_3), 3.97 (s, 2H, CH_2), 6.36 (dd, 1H, J=8.4 Hz, 2.4 Hz, H-4'), 6.44 (t, 1H, H-2'), 6.51 (dd, 1H, J=8.4 Hz, 2 Hz, H-6'), 7.09 (t, 1H, H-5'), 7.47-7.54 (m, 2H, H-5,6), 8.03 (dd, 1H, J=6.8 Hz, 2 Hz, H-4), 8.11 (d, 1H, J=7.6 Hz, H-7), 8.22 (s, 1H, H-3). Carbon NMR (DMSO-d_6, 100 MHz) δ: 48.09 (piperazine-a), 51.02 (OCH_3), 52.05 (piperazine-b), 54.83 (CH_2),

101.61, 104.21, 108.12, 122.90, 124.11, 125.33, 125.44, 126.94, 127.28, 129.57, 138.83, 139.97, 152.24, 160.15, 160.88, 163.73. Mass (ESI) *m/z*: 408.10 [M+H+1].

2-(Benzo[b]thiophen-2-yl)-5-((4-(2-fluorophenyl)piperazin-1-yl)methyl)-1,3,4-oxadiazole (4c)

Yield: 40%. Mp: 175 °C. Proton NMR (DMSO-d_6) δ: 2.72 (t, 4H, H-b), 3.04 (t, 4H, H-a), 3.99 (s, 2H, CH_2), 6.92-7.13 (m, 4H, aromatic protons), 7.47-7.55 (m, 2H, H-5,6), 8.03 (dd, 1H, J=6.8 Hz, 1.6 Hz, H-4), 8.11 (d, 1H, J=8 Hz, H-7), 8.23 (s, 1H, H-3). Carbon NMR (DMSO-d_6, 100 MHz) δ: 49.96 (piperazine-a), 51.02 (CH_2), 52.11 (piperazine-b), 115.88, 119.26, 122.36, 122.90, 124.12, 124.78, 125.39, 126.94, 127.29, 138.84, 139.68, 139.97, 153.70, 156.13, 160.88, 163.73. Mass (ESI) *m/z*: 396.0 [M+H+1].

2-((4-Methylpiperazin-1-yl)methyl)-5-(thiophen-2-yl)-1,3,4-oxadiazole (8a)

Yield: 81%. Mp: 75 °C. Proton NMR (DMSO-d_6) δ: 2.13 (s, 3H, CH_3), 2.32 (bs, 4H, H-a), 2.49 (t, 4H, H-b), 3.83 (s, 2H, CH_2), 7.28 (dd, 1H, J=4.8 Hz, 3.2 Hz), 7.82 (dd, 1H, J=4 Hz, 1.2 Hz), 7.94 (dd, 1H, J=4 Hz, 1.2 Hz). Carbon NMR (DMSO-d_6, 100 MHz) δ: 45.80 (CH_3), 50.25 (CH_2), 52.02 (piperazine-b), 54.20 (piperazine-a), 124.0, 128.25, 130.25, 131.85, 160.50, 163.10. Mass (ESI) *m/z*: 265.46 [M+H].

2-((4-(3-Methoxyphenyl)piperazin-1-yl)methyl)-5-(thiophen-2-yl)-1,3,4-oxadiazole (8b)

Yield: 30%. Mp: 100 °C. Proton NMR (DMSO-d_6) δ: 2.65 (t, 4H, H-b), 3.14 (t, 4H, H-a), 3.69 (s, 3H, CH_3), 3.92 (s, 2H, CH_2), 6.35 (dd, 1H, J=8 Hz, 2 Hz, H-4'), 6.43 (t, 1H, H-2'), 6.50 (dd, 1H, J=8 Hz, 2 Hz, H-6'), 7.08 (t, 1H, H-5'), 7.29 (dd, 1H, J=4.4 Hz, 4 Hz), 7.83 (dd, 1H, J=3.6 Hz, 1.2 Hz), 7.94 (dd, 1H, J=4.8 Hz, 1.2 Hz). Carbon NMR (DMSO-d_6, 100 MHz) δ: 48.08 (piperazine-a), 50.96 (OCH_3), 52.05 (piperazine-b), 54.83 (CH_2), 101.61, 104.22, 108.13, 124.25, 128.75, 129.57, 130.32, 131.56, 152.25, 160.15, 160.76, 163.01. Mass (ESI) *m/z*: 357.63 [M+H].

2-((4-(2-Fluorophenyl)piperazin-1-yl)methyl)-5-(thiophen-2-yl)-1,3,4-oxadiazole(8c)

Yield: 45%. Mp: 127 °C. Proton NMR (DMSO-d_6) δ: 2.67 (t, 4H, H-b), 3.00 (t, 4H, H-a), 3.91 (s, 2H, CH_2), 6.91-7.11 (m, 4H), 7.27 (dd, 1H, J=4.8 Hz, 4 Hz), 7.81 (dd, 1H, J=4 Hz, 1.2 Hz), 7.93 (dd, 1H, J=4 Hz, 1.2 Hz). Carbon NMR (DMSO-d_6, 100 MHz) δ: 49.86 (piperazine-a), 50.88 (CH_2), 52.04 (piperazine-b), 115.80, 119.18, 122.28, 124.18, 124.70, 128.66, 130.24, 131.47, 139.61, 153.63, 156.05, 160.67, 162.92. Mass (ESI) *m/z*: 345.57 [M+H].

Molecular properties prediction

Molecular properties of the synthesized compounds and bioactivity scores were predicted by the Mol inspiration online tool (28). Druglikeness scores were calculated by the molsoft program (29).

Molecular Docking

The X-ray crystallographic structures of the target proteins EGFR (PDB ID: 1xkk), FAK (PDB ID: 2etm), and VEGFR-2 (PDB ID: 3VHE) were retrieved from the Protein Database (PDB, http://www.rcsb.org). The chemical structures of the compounds were constructed, then they were energetically minimized. Native ligand and waters were extracted from the protein, and the polar hydrogen was added to the proteins. The grid boxes of EGFR and FAK, VEGFR-2 were created with spacing 48x40x48 and 30x30x30, respectively. The docking study was performed using AutoDock vina 1.1.2 (30). The binding energy of the compounds and interactions with protein were evaluated.

RESULT AND DISCUSSION

Chemistry

Synthesis of the target compounds (**4a-c**, **8a-c**) derivatives is depicted in Scheme 1. Firstly, the methyl esters (**1** and **5**) were prepared by esterification of appropriate carboxylic acid in the presence of H_2SO_4 in methanol (31). Hydrazide derivatives (**2** and **6**) were obtained by the reaction of esters (**1** and **5**) with hydrazine hydrate in methanol (32). Hydrazides were refluxed with chloroacetic acid in phosphorous oxychloride to afford 2-(benzo[*b*]thiophen-2-yl)-5-(chloromethyl)-1,3,4-oxadiazole (**3**) and 2-(chloromethyl)-5-(thiophen-2-yl)-1,3,4-oxadiazole (**7**). Final products (**4a-c**, **8a-c**) were prepared by the alkylation reactions of compound **3** and **7** with appropriate piperazine derivatives in the presence of K_2CO_3 and KI (33).

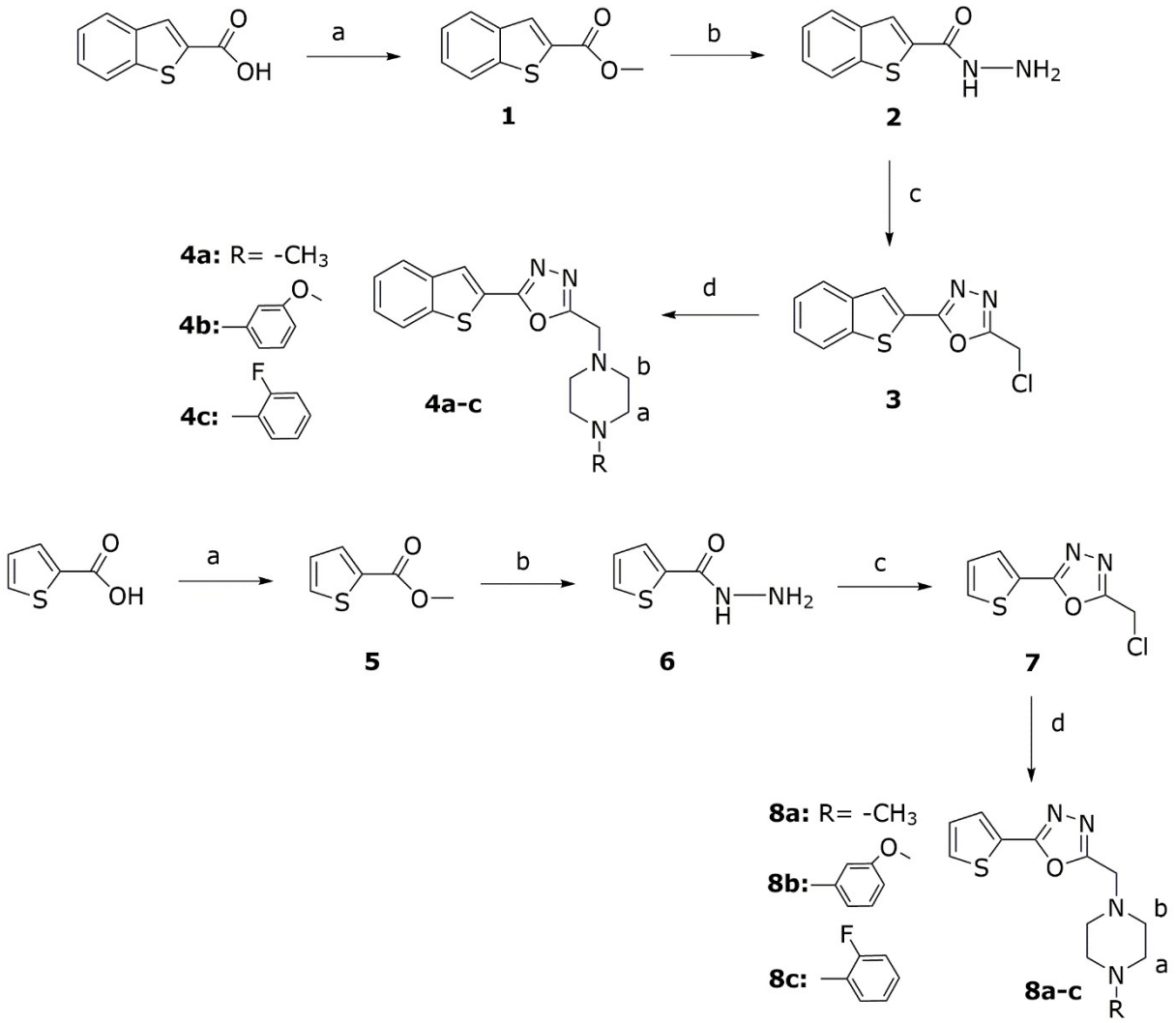

Scheme 1. A synthesis method of compounds **4a-c** and **8a-c**. Reaction conditions: (a) methanol, concd. H_2SO_4 (0.1 mL) (b) hydrazine hydrate, methanol, reflux (c) chloroacetic acid, phosphoryl chloride, reflux (d) K_2CO_3, KI, appropriate piperazine derivatives, acetone, reflux.

^{1}H NMR, ^{13}C NMR, and MS analysis were performed to characterize the compounds. ^{1}H NMR spectra of the compounds containing phenylpiperazine derivatives (**4b-c**, **8b-c**) showed a triplet at *δ* 2.65-2.72 and 3.0-3.15 ppm indicating the presence of piperazine protons–b and –a, respectively. In the compounds bearing *N*-methylpiperazine moiety (**4a** and **8a**), piperazine protons-a showed the peak in the upfield region (2.30-2.32 ppm) due to the shielding effect of the methyl group. Chemical shift between *δ* 3.83 to 3.99 ppm showed by all compounds represent the protons of CH_2. Compound **4a-c** exhibited multiplet at *δ* 7.44-7.55 and singlet peak at *δ* 8.19-8.23 ppm due to H-5,6 and H-3 protons of benzo[*b*]thiophene ring, respectively. Chemical shift between *δ* 8.01-8.03 ppm showed by compounds **4a-c** represents the H-4 proton. The peak belonging H-7 proton of benzo[*b*]thiophene ring was observed in the downfield region (8.08-8.11 ppm) due to nearby sulfur atom of thiophene ring. Compound **8a-c** showed three double doublets peak between *δ* 7.27-7.94 ppm due to the presence of the thiophene ring. ^{13}C NMR spectra of the target compounds (**4b-b**, **8b-c**) displayed peaks at *δ* 48.08-54.40, and *δ* 51.97-52.11 ppm representing piperazine carbon–a and –b. The peaks between *δ* 50.88-54.83 ppm indicate the presence of CH_2 carbons. Compound **4a** and **8a** with *N*-methylpiperazine moiety showed peaks at *δ* 45.75 and 45.80 ppm due to CH_3 carbon, respectively. Compound **4b** and **8b** displayed peaks at *δ*

51.02 and 50.96 ppm, indicating the presence of OCH_3, respectively.

Molecular properties prediction and drug-likeness

Some molecular properties, which are shown in Table 1, were calculated using Molinspiration online calculation software (28). The predicted values are given in Table 1. All the compounds meet the LogP criteria. Calculation of %ABS was done with equation %ABS = 109 − (0.345 x TPSA) (34). All synthesized compounds possess the good %ABS value of 90.15 and 93.33% and acceptable *n*OHNH (≤5) and *n*ON (≤10) number. Also, NROTB (≤10) of the compounds were found as 3-5, providing moderate flexibility to the compounds (35). MW of the compounds was found less than 500. Druglikeness model score was predicted by MolSoft software (29) and shown in Table 1. Drug-like candidate compounds should have a value of more than zero. Compounds **4b** and **8b** possess the highest drug-likeness score of 0.31 and 0.33, respectively.

Table 1. Predicted molecular properties and drug-likeness scores of the target compound (**4a-c**, **8a-c**).

Cpd	MW[a]	Volume	%ABS[b]	TPSA[c]	NROTB[d]	*n*ON[e]	*n*OHNH[f]	LogP[g]	*n*violations	Drug likeness score
Rule	>500	-	-	-	-	≤10	≤5	≤5	≥1	-
4a	314.41	278.71	93.33	45.40	3	5	0	2.15	0	0.14
4b	406.51	359.10	90.15	54.63	5	6	0	3.88	0	0.31
4c	394.48	338.49	93.33	45.40	4	5	0	3.96	0	0.15
8a	264.35	234.72	93.33	45.40	3	5	0	0.84	0	0.07
8b	356.45	315.11	90.15	54.63	5	6	0	2.57	0	0.33
8c	344.42	294.49	93.33	45.40	4	5	0	2.65	0	0.14

[a] MW: Molecular weight; [b] %ABS: Percentage absorption; [c]TPSA: Topological polar surface area; [d] NROTB: Number of rotatable bonds; [e] *n*ON: Number of hydrogen acceptors; [f] *n*OHNH: Number of hydrogen donors; [g] LogP: Log octanol/water partition coefficient.

Bioactivity score prediction and molecular docking

Bioactivity scores, which are given in Table 2, were predicted by Molinspiration online calculation software (28). If the bioactivity score of the compound is >0 or -0.5-0 or <0, it can be active or moderate or inactive, respectively (36). Synthesized compounds showed the acceptable kinase inhibitor scores (>0 or -0.5-0) with compound **4a-c**; **8a-c** suggested that these compounds might possess kinase inhibitor activity. So, EGFR, FAK, and VEGFR-2 kinases, which are reported as targets for many oxadiazole derivatives (21-24), were selected as putative targets for synthesized compounds. Molecular docking studies were performed using Autodock vina to present the binding interactions between synthesized compounds and the active site of EGFR, FAK, and VEGFR-2 kinases.

Table 2. Bioactivity scores prediction of the target compounds (**4a-c**, **8a-c**).

Cpd	GPCRL	ICM	KI	NRL	PI	EI
4a	-0.02	-0.37	0.14	-0.44	-0.11	-0.03
4b	-0.07	-0.41	0.05	-0.37	-0.16	-0.14
4c	-0.05	-0.35	0.08	-0.40	-0.10	-0.11
8a	-0.42	-0.53	-0.35	-1.04	-0.54	-0.27
8b	-0.24	-0.53	-0.19	-0.65	-0.33	-0.30
8c	-0.22	-0.46	-0.15	-0.70	-0.27	-0.27

GPCRL: G protein-coupled receptor ligand; ICM: ion channel modulator; KI: kinase Inhibitor; NRL: nuclear receptor ligand; PI: protease inhibitor; EI: enzyme inhibitor.

The docking method was optimized by re-docking of co-crystallized ligands into the binding site of target proteins. The re-docked ligands of EGFR, FAK, and VEGFR-2 kinases were superimposed on native ligands with RMSD values of 1.42, 0.7, and 0.5 Å, respectively. According to docking results, all compounds occupied into the binding site of VEGFR-2 and formed the hydrogen bond between oxadiazole ring and Asp1046 amino acid. The docking results, binding free energy, hydrogen bond distance, and angles were shown in Table 3. The binding model of compound **4b,** which has the lowest binding

free energy (ΔGb=-11.2 kcal/mol) in the active site of VEGFR-2 was depicted in Figure 2. Otherwise, compounds did not show interaction with the key residue of EGFR (Met793 and Thr854) and FAK kinase (Cys502) active sites. Docking results of compounds with EGFR and FAK kinases were given in supplementary material (Figure S1, Table S1-S2).

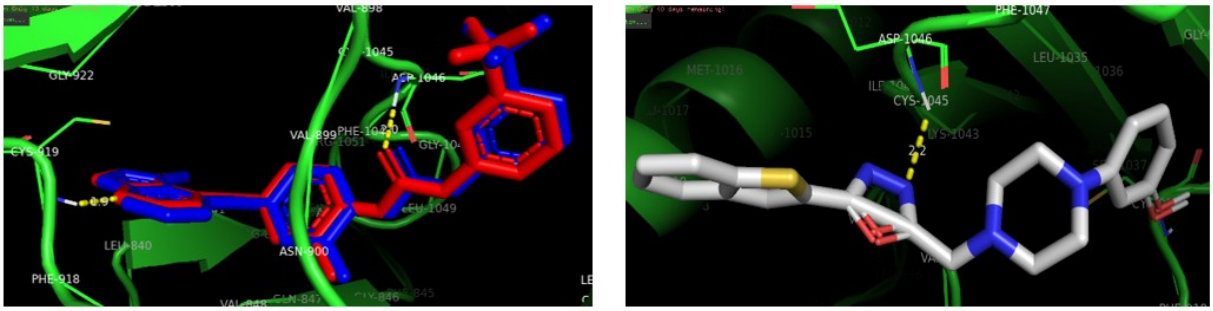

Figure 2. Superposition of co-crystallized (blue) and docked (red) conformations of the reference ligand (left). Predicted binding mode of compound **4b** in the active site of VEGFR-2 (PDB code: 3VHE) (right). Hydrogen bonds were shown as yellow dashed lines. Figure was generated using PyMOL.

Table 3. The docking results of the compounds.

Compound	ΔGb[a] (kcal/mol)	Hydrogen bonds			
		Atom of compound	Amino acid	Distance (Å) D-H.....A	Angle (°)
4a	-9.1	Oxadiazole-O	Asp1046-NH	1.9	163.7
4b	-11.2	Oxadiazole-N4	Asp1046-NH	2.2	136.3
4c	-11.0	Oxadiazole-O	Asp1046-NH	2.2	148.4
8a	-6.9	Oxadiazole-N3	Asp1046-NH	2.2	128.4
8b	-8.7	Oxadiazole-N4	Asp1046-NH	2.2	140.3
8c	-9.4	Oxadiazole-O	Asp1046-NH	2.2	151.0
Native ligand		Urea-N PP-N4 Urea-O	Glu885-O Cyc919-NH Asp1046-NH		
Docked ligand	-12.6 RMSD[b]:0.5	Urea-O PP-N4	Asp1046-NH Cyc919-NH	2.0 1.9	161.9 162.4

[a]Binding free energy, [b]root-mean-square deviation

CONCLUSION

In this study, 2-(benzo[*b*]thiophen-2-yl)-5-((4-substituted-piperazin-1-yl)methyl)-1,3,4-oxadiazole (**4a-c**) and 2-((4-substituted-piperazin-1-yl)methyl)-5-(thiophen-2-yl)-1,3,4-oxadiazole derivatives (**8a-c**) were synthesized and molecular properties and bioactivity score were predicted. All compounds obeyed the Lipinski's rules and showed good drug-likeness scores. The best bioactivity prediction scores of compounds were found as a kinase inhibitor. Moreover, hydrogen bonding interactions of the compounds with VEGFR-2 kinase active site were found by molecular docking study, suggesting possible *in vitro* inhibitor activities of these compounds towards VEGFR-2 kinase.

ACKNOWLEDGEMENTS

Ankara University supported this research. We thank Prof. Hakan Goker from Central Instrumentation Laboratory of Faculty of Pharmacy, Ankara University, for NMR and Mass analyses.

REFERENCES

1. Glomb T, Szymankiewicz K, S´wiatek P. Anti-cancer activity of derivatives of 1,3,4-oxadiazole. Molecules. 2018;23,33-61. Doi:10.3390/molecules23123361.

2. Boström J, Hogner A, Llinàs A, Wellner E, Plowright AT. Oxadiazoles in Medicinal Chemistry. Journal of Medicinal Chemistry. 2012;55:1817−1830. Doi:10.1021/jm2013248.

3. Zhang HZ, Zhao ZL, Zhou CH. Recent advance in oxazole-based medicinal chemistry.

European Journal of Medicinal Chemistry. 2018;144:444-492. Doi:10.1016/j.ejmech.2017.12.044.

4. Akhtar J, Khan AA, Ali Z, Haider R, Shahar Yar M. Structure-activity relationship (SAR) study and design strategies of nitrogen-containing heterocyclic moieties for their anticancer activities. 2017;125:143-189. Doi: 10.1016/j.ejmech.2016.09.023.

5. James ND, Growcott JW. Zibotentan. Drugs of the Future. 2009;34(8):624-633. Doi:10.1358/dof.2009.34.8.1400202.

6. Jones AM, Helm JM. Emerging treatments in cystic fibrosis. Drugs. 2009;69:1903−1910. Doi:10.2165/11318500-000000000-00000.

7. Rasool I, Ahmad M, Khan ZA, Mansha A, Maqbool T, Zahoor AF, Aslam S. Recent advancements in oxadiazole-based anticancer agents. Tropical Journal of Pharmaceutical Research.2017;16:723-733. Doi:10.4314/tjpr.v16i3.30.

8. Khan I, Ibrar A, Abbas N. Oxadiazoles as Privileged Motifs for Promising Anticancer Leads: Recent Advances and Future Prospects. Archiv der Pharmazie. 2014;347:1-20. Doi:10.1002/ardp.201300231.

9. Bajaj S, Asati V, Singh J, Roy PP. 1,3,4-Oxadiazoles: An emerging scaffold to target growth factors, enzymes and kinases as anticancer agents. European Journal of Medicinal Chemistry. 2015;97:124-141. Doi:10.1016/j.ejmech.2015.04.051.

10. Ouyang X, Piatnitski EL, Pattaropong V, Chen X, Hai-Ying H, et al. Synthesis, inhibition of tubulin polymerization, and activity in tumor cell lines. Bioorganic and Medicinal Chemistry Letters. 2006;16:1191-1196. Doi:10.1016/j.bmcl.2005.11.094.

11. Zhang K, Wang P, Xuan LN, Fu XY, Jing F, Li S, Liu YM, Chen BQ, Synthesis and antitumor activities of novel hybrid molecules containing 1,3,4-oxadiazole and 1,3,4-thiadiazole bearing Schiff base moiety. Bioorganic and Medicinal Chemistry Letters. 2014;24:5154-5156. Doi:10.1016/j.bmcl.2014.09.086.

12. Pidugu VR, Yarla NS, Pedada SR, Kalle AM, Satya AK. Design and synthesis of novel hdac8 ınhibitory 2,5-disubstituted-1,3,4-oxadiazoles containing glycine and alanine hybrids with anti cancer activity. Bioorganic Medicinal Chemistry. 2016;24:5611–5617. Doi:10.1016/j.bmc.2016.09.022.

13. Mohan CD, Anilkumar NC, Rangappa S, Shanmugam MK, Mishra S, Chinnathambi A, Alharbi SA, Bhattacharjee A, Sethi G, Kumar AP, Rangappa KS. Novel 1,3,4-oxadiazole induces anticancer activity by targeting nf-κb in hepatocellular carcinoma cells. Frontiers in Oncology. 2018;8:42. Doi:10.3389/fonc.2018.00042.

14. Abou-Seri SM. Synthesis and biological evaluation of novel 2,4’-bis substituted diphenylamines as anticancer agents and potential epidermal growth factor receptor tyrosine kinase inhibitors. European Journal of Medicinal Chemistry. 2010;45:4113–4121. Doi:10.1016/j.ejmech.2010.05.072.

15. Sun L, Ren SZ, Lu XY, Li JJ, Shen FQ, Xu C, Zhu HL. Discovery of a series of 1,3,4-oxadiazole-2(3h)-thione derivatives containing piperazine skeleton as potential Fak inhibitors. Bioorganic Medicinal Chemistry. 2017;25:2593–2600. Doi:10.1016/j.bmc.2017.03.038.

16. Kiselyov AS, Semenova M, Semenov VV, Milligan D. Inhibitors of VEGF receptors-1 and -2 Based on the 2-((pyridin-4-yl)ethyl)pyridine Template. Bioorganic Medicinal Chemistry Letters. 2006;16:1913–1919. Doi:10.1016/j.bmcl.2005.12.090.

17. Cai Z-W, Wei D, Borzilleri RM, Qian L, Kamath A, Mortillo S, Wautlet B, Henley BJ, Jeyaseelan R, Tokarski J, Hunt JT, Bhide RS, Fargnoli J, Lombardo LJ. Synthesis, SAR, and Evaluation of 4-[2,4-Difluoro-5-(cyclopropylcarbamoyl) phenylamino] pyrrolo[2,1-f][1,2,4]triazine-based VEGFR-2 Kinase Inhibitors. Bioorganic Medicinal Chemistry Letters. 2008;18:1354–1358. Doi:10.1016/j.bmcl.2008.01.012.

18. Piatnitski Chekler EL, Kiselyov AS, Ouyang X, Chen X, Pattaropong W, Wang Y, Tuma MC, Doody JF. Discovery of dual VEGFR-2 and tubulin inhibitors with in vivo efficacy. ACS Medicinal Chemistry Letters. 2010;1:488-492. Doi:10.1021/ml1001568.

19. Hughes TV, Xu G, Wetter SK, Connolly PJ, Emanuel SL, Karnachi P, Pollack SR, Pandey N, Adams M, Moreno-Mazza S, Middleton SA, Greenberger LM. A novel 5-[1,3,4-oxadiazol-2-yl]-N-aryl-4,6-pyrimidine diamine having dual

EGFR/HER2 kinase activity: Design, synthesis, and biological activity. Bioorganic Medicinal Chemistry Letters. 2008;18:4896–4899. Doi:10.1016/j.bmcl.2008.07.057.

20. Dokla EME, Fang C-S, Abouzid KAM, Chen CS. 1,2,4-Oxadiazole derivatives targeting EGFR and c-Met degradation in TKI resistant NSCLC. European Journal of Medicinal Chemistry. 2019;182:111607. Doi:10.1016/j.ejmech.2019.111607

21. Fathi MA, Abd El-Hafeez AA, Abdelhamid D, Abbas SH, Montano MM, Abdel-Aziz M. 1,3,4-oxadiazole/chalcone Hybrids: Design, synthesis, and ınhibition of leukemia cell growth and egfr, src, IL-6 and stat3 activities. Bioorganic Chemistry. 2019;84:150–163. Doi:10.1016/j.bioorg.2018.11.032.

22. Altıntop MD, Sever B, Çiftçi GA, Turan-Zitouni G, Kaplancıklı ZA, Özdemir A. Design, synthesis, in vitro and in silico evaluation of a new series of oxadiazole-based anticancer agents as potential Akt and Fak ınhibitors. European Journal of Medicinal Chemistry. 2018;155:905–924. Doi:10.1016/j.ejmech.2018.06.049.

23. Ruel R, Thibeault C, L'Heureux A, Martel A, Cai ZW, Wei D, Qian L, Barrish JC, Mathur A, D'Arienzo C, et al. Discovery and preclinical studies of 5-isopropyl-6-(5-methyl-1,3,4 -oxadiazol-2-yl)-N-(2-methyl-1H-pyrrolo[2,3-b]pyridin-5-yl)pyrrolo [2,1-f][1,2,4]triazin-4-amine (BMS-645737), an in vivo active potent VEGFR-2 inhibitor. Bioorganic Medicinal Chemistry Letterrs. 2008;18:2985–2989. Doi:10.1016/j.bmcl.2008.03.057

24. Bhanushali U, Kalekar-Joshi S, Kulkarni-Munshi R, Yellanki S, Medishetty R, Kulkarni P, Chelakara RS. Design, synthesis and evaluation of 5-pyridin-4-yl-2-thioxo-[1,3,4] oxadiazol-3-yl derivatives as anti-angiogenic agents targeting VEGFR-2. Anticancer Agents Medicinal Chemistry. 2017;17:67–74. Doi:10.2174/1871520615666160504094222

25. Feinstein A, Gore PH, Reed, GL. Alkaline hydrolysis of the methyl esters of benzo[b] furan-2- and 3-carboxylic acid, benzo[b]thiophene-2- and 3-carboxylic acid, and indole-2- and 3-carboxylic acid. Journal of the Chemical Society [Section] B: Physical Organic. 1969;3:205-207.

26. Kovalenko SI, Antypenko LM, Bilyi AK, Kholodnyak SV, Karpenko OV, Antypenko OM, Mykhaylova NS, Los TI, Kolomoets OS. Synthesis and anticancer activity of 2-(alkyl-, alkaryl-, aryl-, hetaryl-)[1,2,4]triazolo[1,5-c]quinazolines. Scientia Pharmaceutica. 2013;81(2):359-391. Doi:10.3797/scipharm.1211-08.

27. Guo Y, Xu T, Bao C, Liu Z, Fan J, Yang R, Qin S. Design and synthesis of new norfloxacin-1,3,4-oxadiazole hybrids as antibacterial agents against methicillin-resistant Staphylococcus aureus (MRSA). European Journal of Pharmaceutical Sciences. 2019;136:104966. Doi:10.1016/j.ejps.2019.104966.

28. Molinspiration Cheminformatics, Bratislava, Slovak Republic, Available from: http://www.molinspiration.com/services/properties.html

29. Drug-likeness and molecular property prediction, available from: http:// www.molsoft.com/mprop/

30. Trott O, Olson AJ. AutoDock Vina: improving the speed and accuracy of docking with a new scoring function, efficient optimization and multithreading, Journal of Computational Chemistry. 2010;31:455-461. Doi: 10.1002/jcc.21334.

31. Mistry SN, Shonberg J, Draper-Joyce CJ, Herenbrink CK, Michino M, Shi L, Christopoulos A, Capuano B, Scammells PJ, Lane JR. Discovery of a novel class of negative allosteric modulator of the dopamine d2 receptor through fragmentation of a bitopic ligand. Journal of Medicinal Chemistry. 2015;58:6819-6843. Doi: 10.1021/acs.jmedchem.5b00585.

32. Almutairi MS, Zakaria AS, Ignasius PP, Al-Wabli RI, Joe IH, Attia MI. Synthesis, spectroscopic investigations, DFT studies, molecular docking and antimicrobial potential of certain new indole-isatin molecular hybrids: Experimental and theoretical approaches. Journal of Molecular Structure. 2018;1153:333-345. Doi:10.1016/j.molstruc.2017.10.025.

33. Wei Z-Y, Chi K-Q, Wanga K-S, Wub J, Liu L-P, Piao H-R. Design, synthesis, evaluation, and molecular docking of ursolic acid derivatives containing a nitrogen heterocycle as anti-inflammatory agents. Bioorganic and Medicinal Chemistry Letters. 2018;28:1797-1803. Doi:10.1016/j.bmcl.2018.04.021.

34. Zhao YH, Abraham MH, Le J, Hersey A, Luscombe CN, Beck G, Sherborne B, Cooper Rate-limited steps of human oral absorption and QSAR studies. I. Pharmaceutical Research. 2002;19:1446-1457. Doi:10.1023/A:1020444330011

35. Veber DF, Johnson SR, Cheng HY, Smith BR, Ward KW, Kopple KD. Molecular properties that influence the oral bioavailability of drug candidates. Journal of Medicinal Chemitry. 2002;45:2615-2623. Doi:10.1021/jm020017n

36. Jain NK, Chourasia MK, Jain S, Jain SK. Development and characterization of engineered commensal bacteria for the delivery of enzymes. Indian Journal of Pharmaceutical Sciences. 2003;65:113-121.

SUPPLEMENTARY DATA

Synthesis of Novel Oxadiazole Derivatives, Molecular Properties Prediction and Molecular Docking Studies

Zühal KILIC-KURT*

Ankara University, Faculty of Pharmacy, Department of Pharmaceutical Chemistry, Tandogan, Ankara, Turkey

***Corresponding author.** E-mail: zkurt@ankara.edu.tr

NMR and mass spectral analysis of the target compounds

2-(Benzo[b]thiophen-2-yl)-5-((4-methylpiperazin-1-yl)methyl)-1,3,4-oxadiazole (4a)

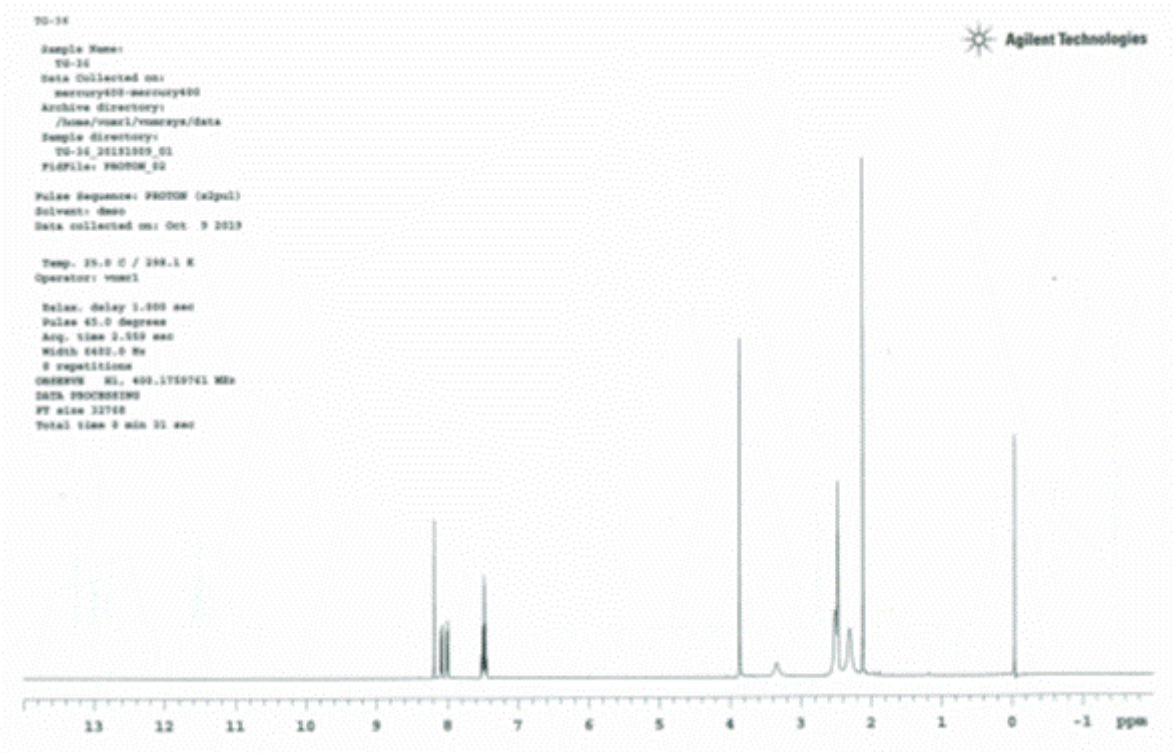

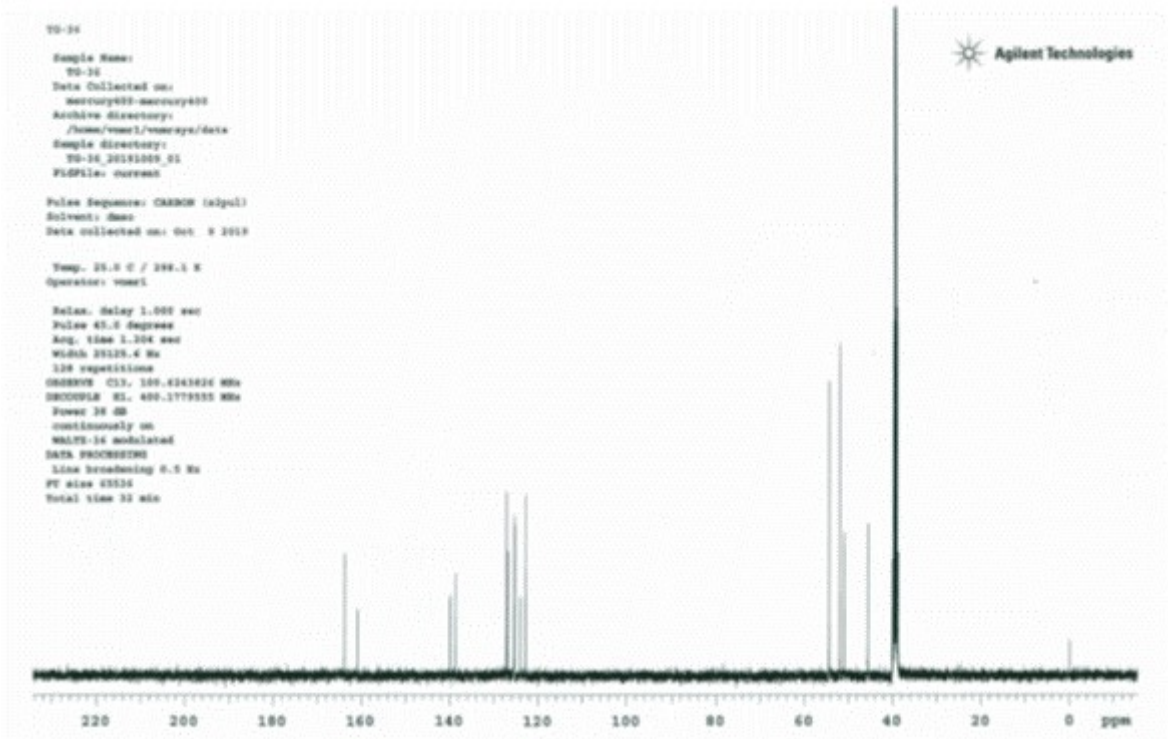
Agilent Technologies
220
200
180
160
140
120
100
80
60
40
20
0
ppm

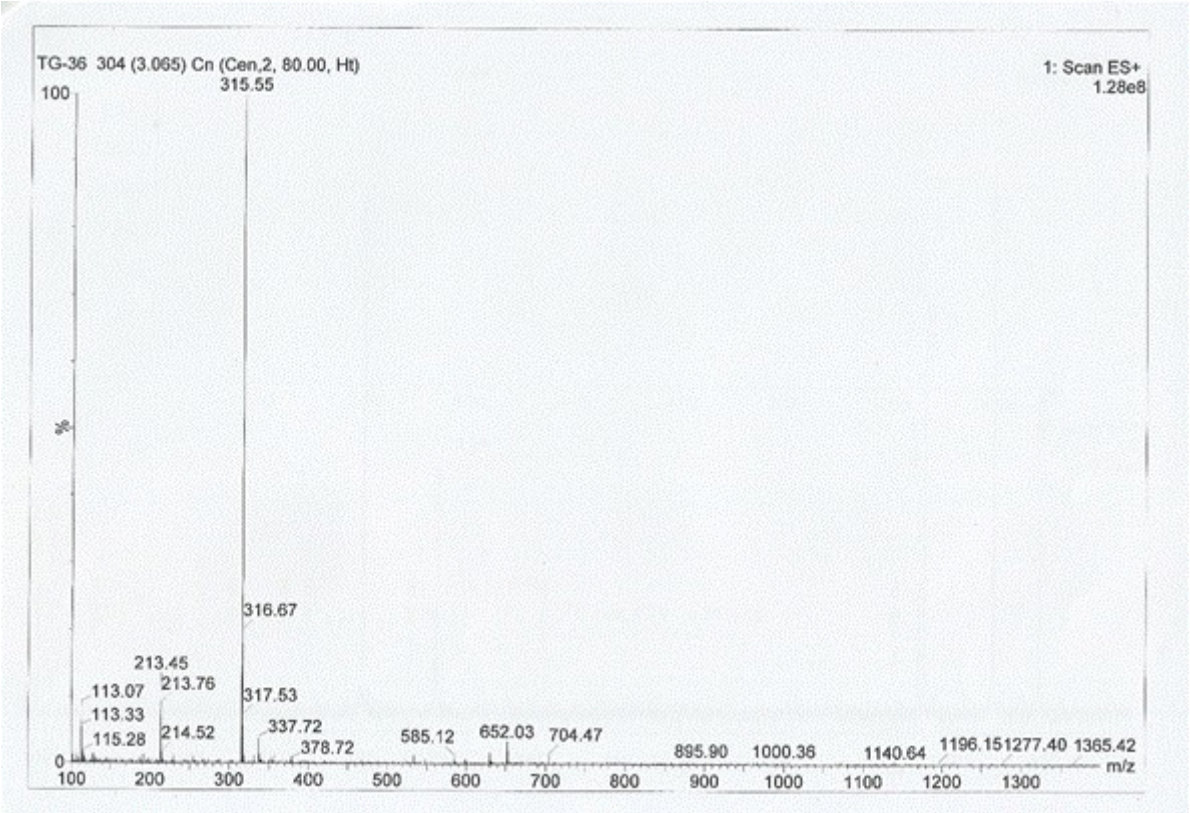
TG-36 304 (3.065) Cn (Cen,2, 80.00, Ht)
1: Scan ES+
1.28e8
100
%
315.55
316.67
213.45
213.76
113.07
113.33
115.28
214.52
317.53
337.72
378.72
585.12
652.03
704.47
895.90
1000.36
1140.64
1196.15
1277.40
1365.42
0
100
200
300
400
500
600
700
800
900
1000
1100
1200
1300
m/z

2-(Benzo[b]thiophen-2-yl)-5-((4-(3-methoxyphenyl)piperazin-1-yl)methyl)-1,3,4-oxadiazole (4b)

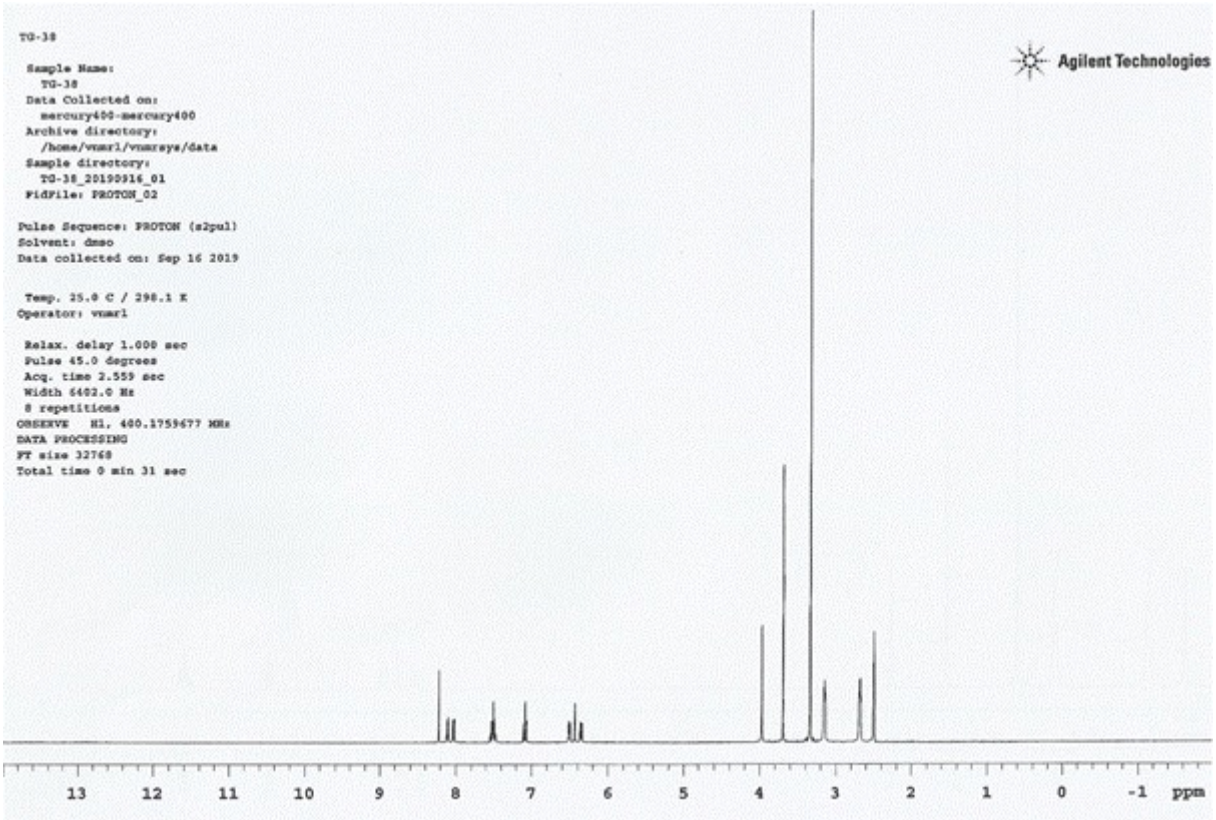

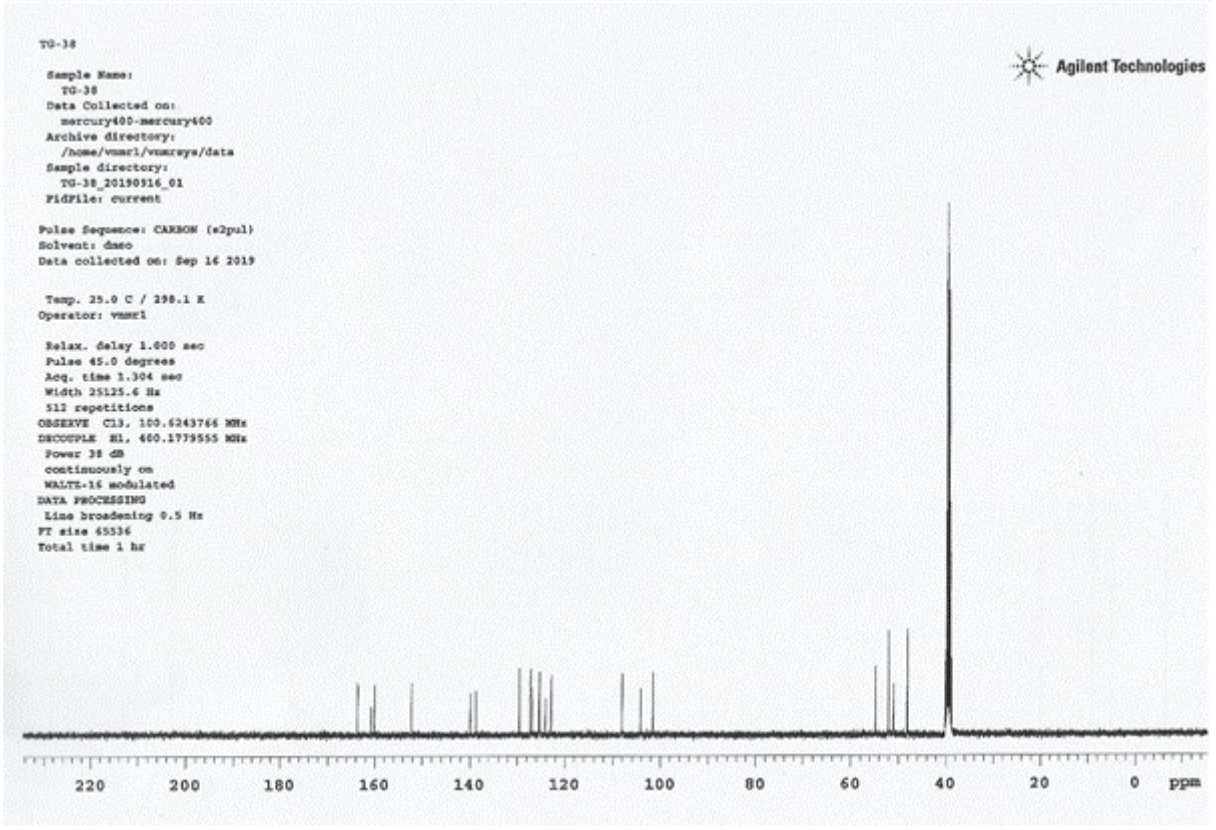

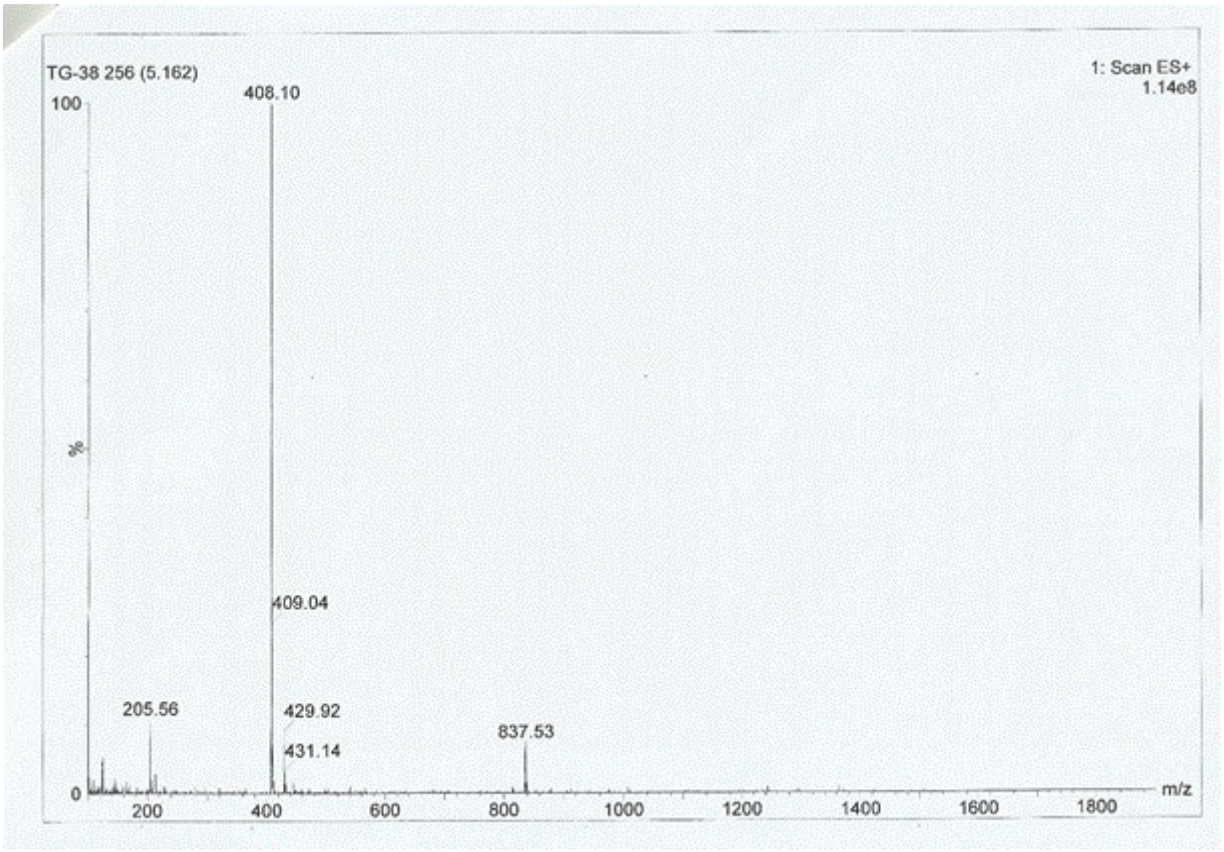

2-(Benzo[b]thiophen-2-yl)-5-((4-(2-fluorophenyl)piperazin-1-yl) methyl)-1,3,4-oxadiazole (4c)

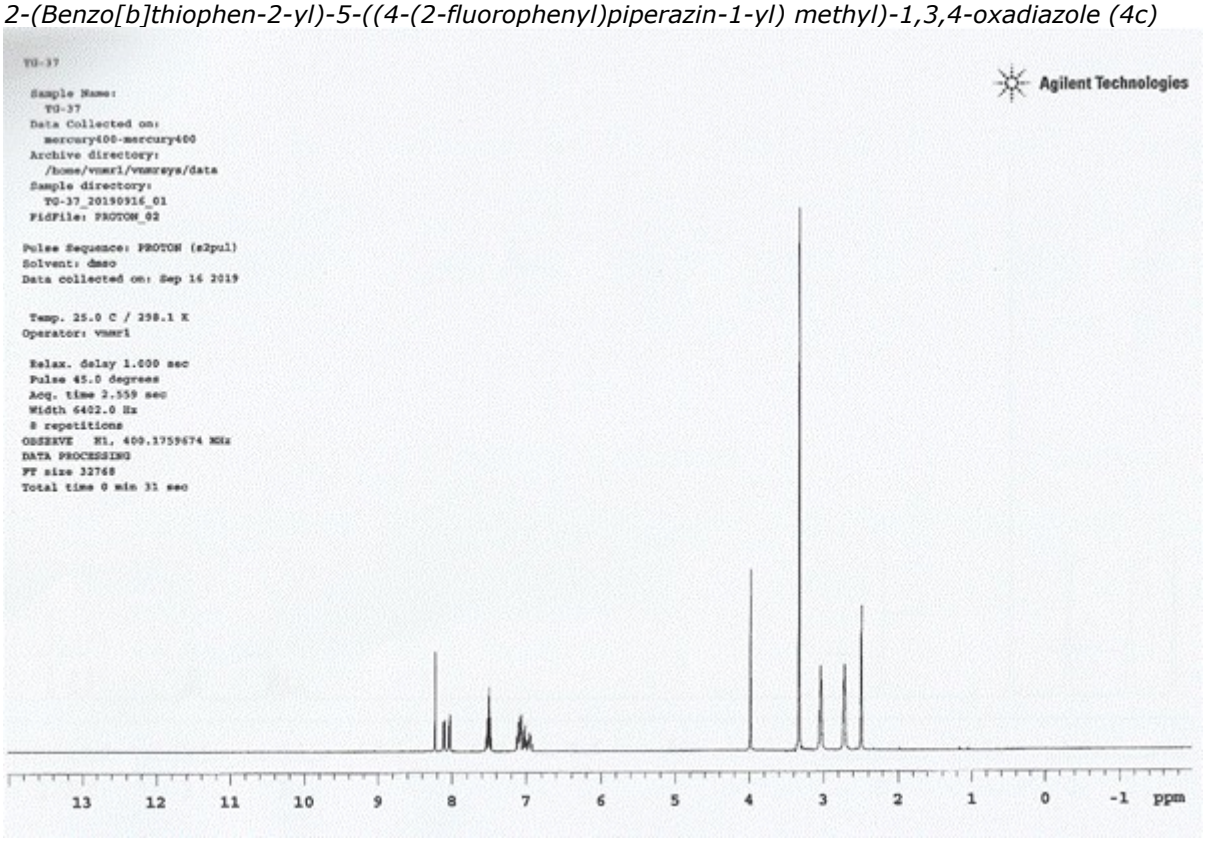

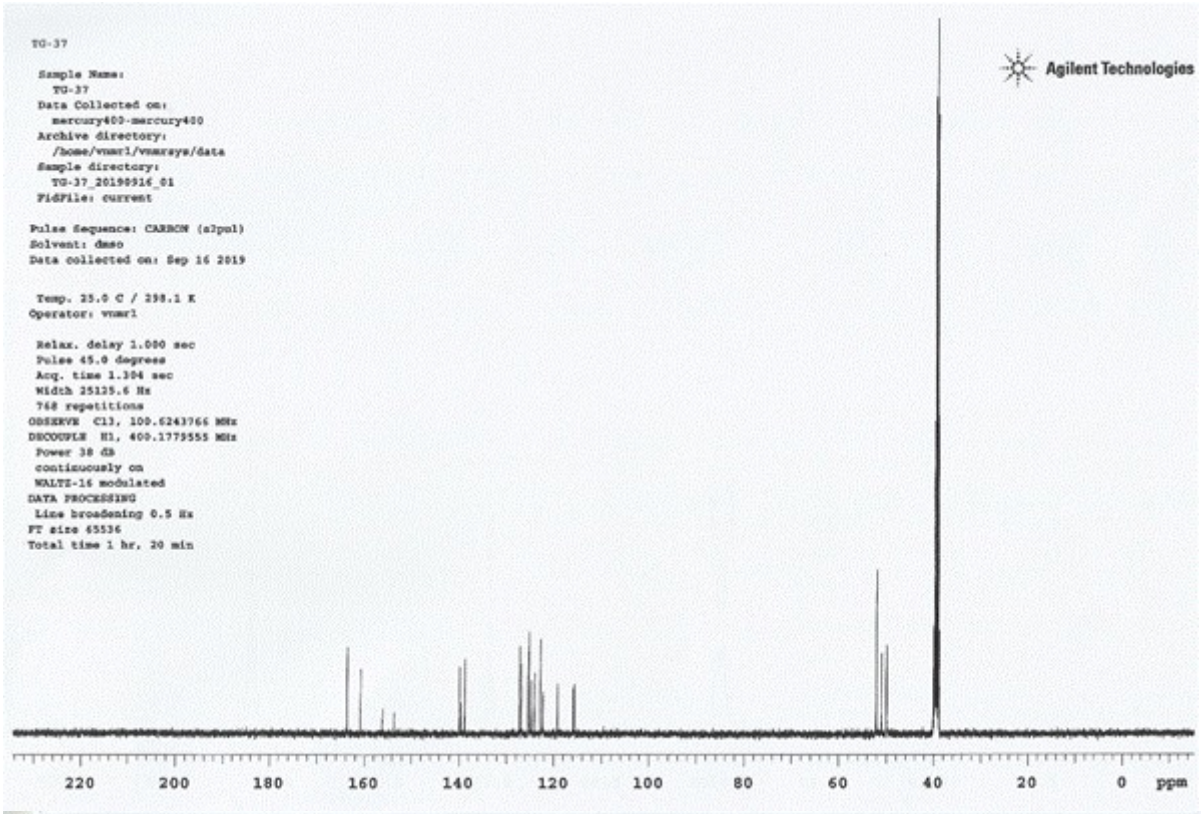
TG-37
Sample Name:
TG-37
Data Collected on:
mercury400-mercury400
Archive directory:
/home/vnmrl/vnmrsys/data
Sample directory:
TG-37_20190916_01
FidFile: current
Pulse Sequence: CARBON (s2pul)
Solvent: dmso
Data collected on: Sep 16 2019
Temp. 25.0 C / 298.1 K
Operator: vnmrl
Relax. delay 1.000 sec
Pulse 45.0 degrees
Acq. time 1.304 sec
Width 25125.6 Hz
768 repetitions
OBSERVE C13, 100.6243766 MHz
DECOUPLE H1, 400.1775555 MHz
Power 38 dB
continuously on
WALTZ-16 modulated
DATA PROCESSING
Line broadening 0.5 Hz
FT size 65536
Total time 1 hr, 20 min
Agilent Technologies
220
200
180
160
140
120
100
80
60
40
20
0
ppm

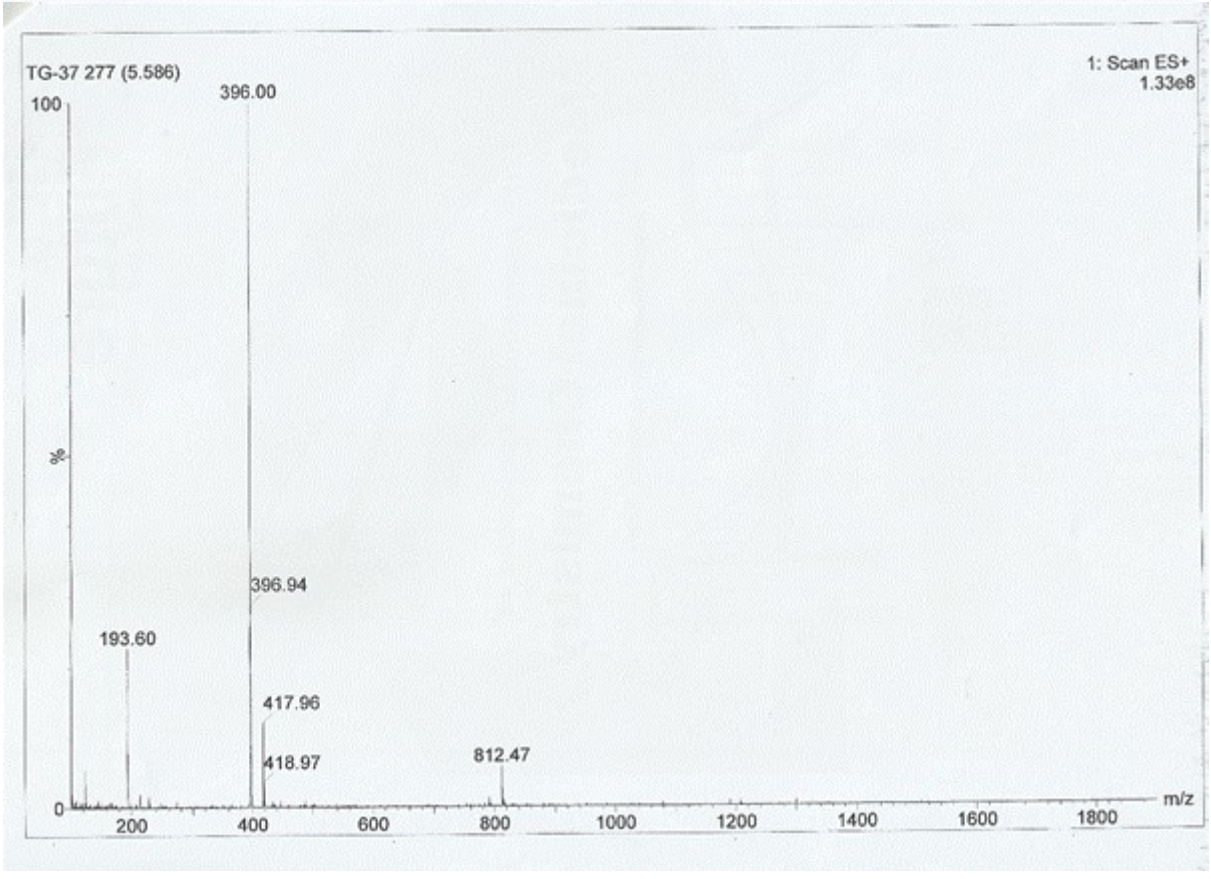
TG-37 277 (5.586)
1: Scan ES+
1.33e8
100
%
0
396.00
396.94
193.60
417.96
418.97
812.47
200
400
600
800
1000
1200
1400
1600
1800
m/z

2-((4-Methylpiperazin-1-yl)methyl)-5-(thiophen-2-yl)-1,3,4-oxadiazole (8a)

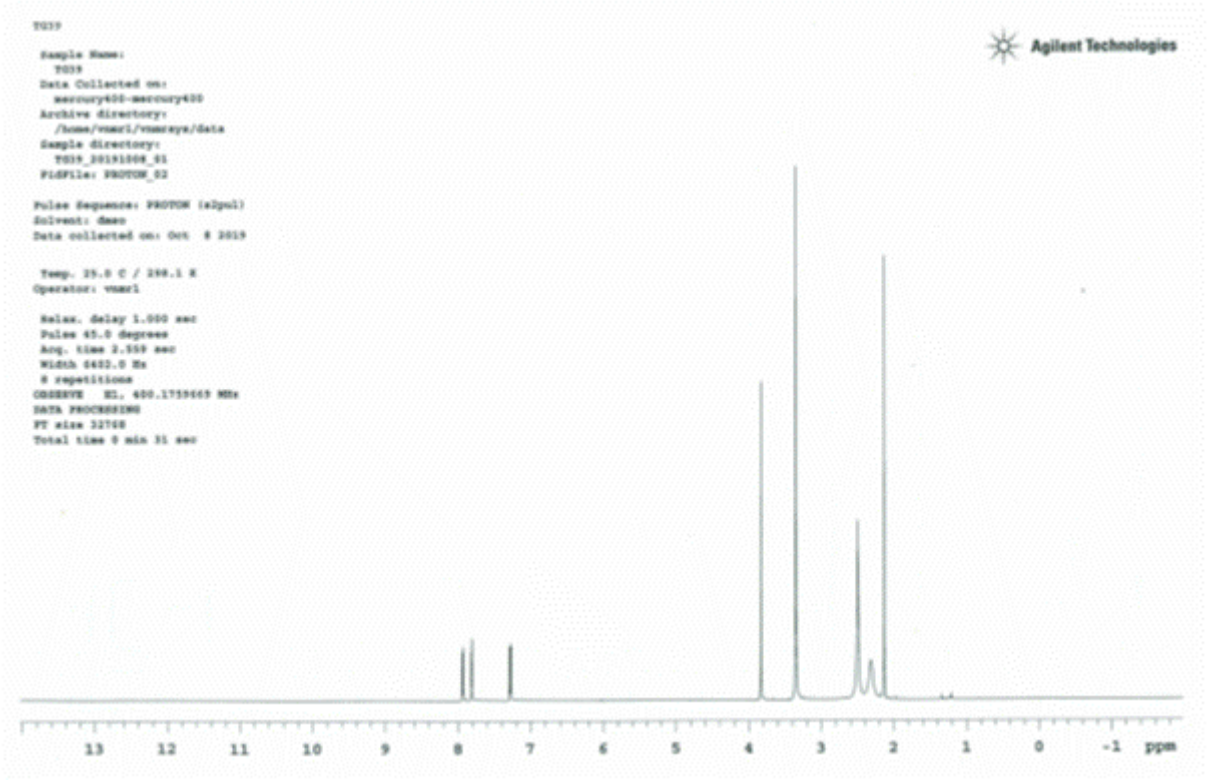

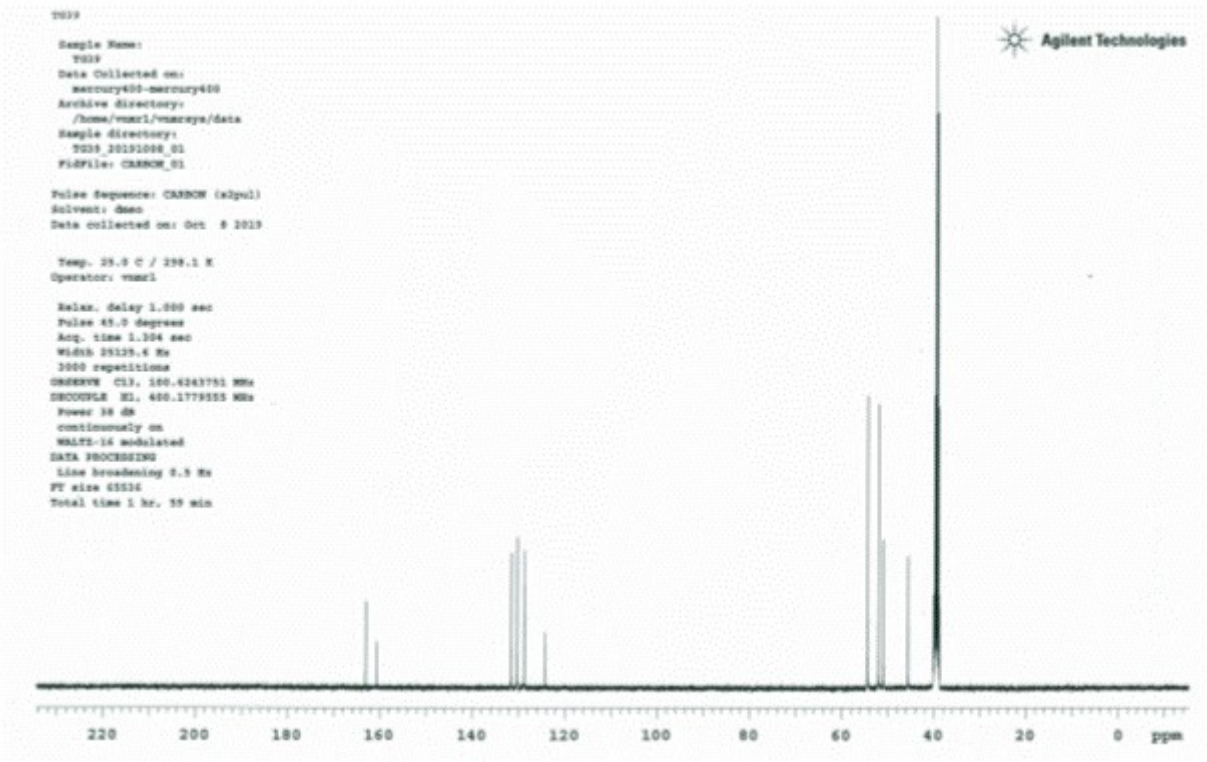

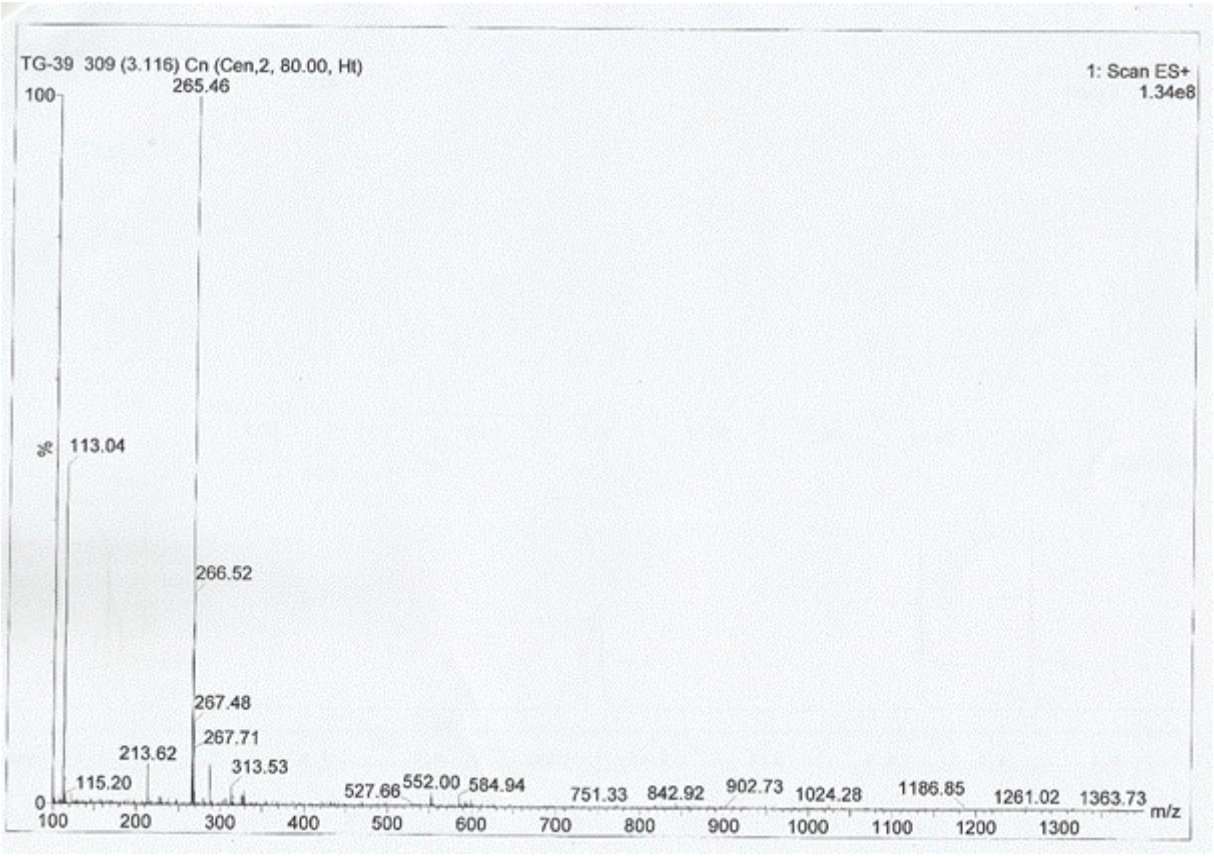

2-((4-(3-Methoxyphenyl)piperazin-1-yl)methyl)-5-(thiophen-2-yl)-1,3,4-oxadiazole (8b)

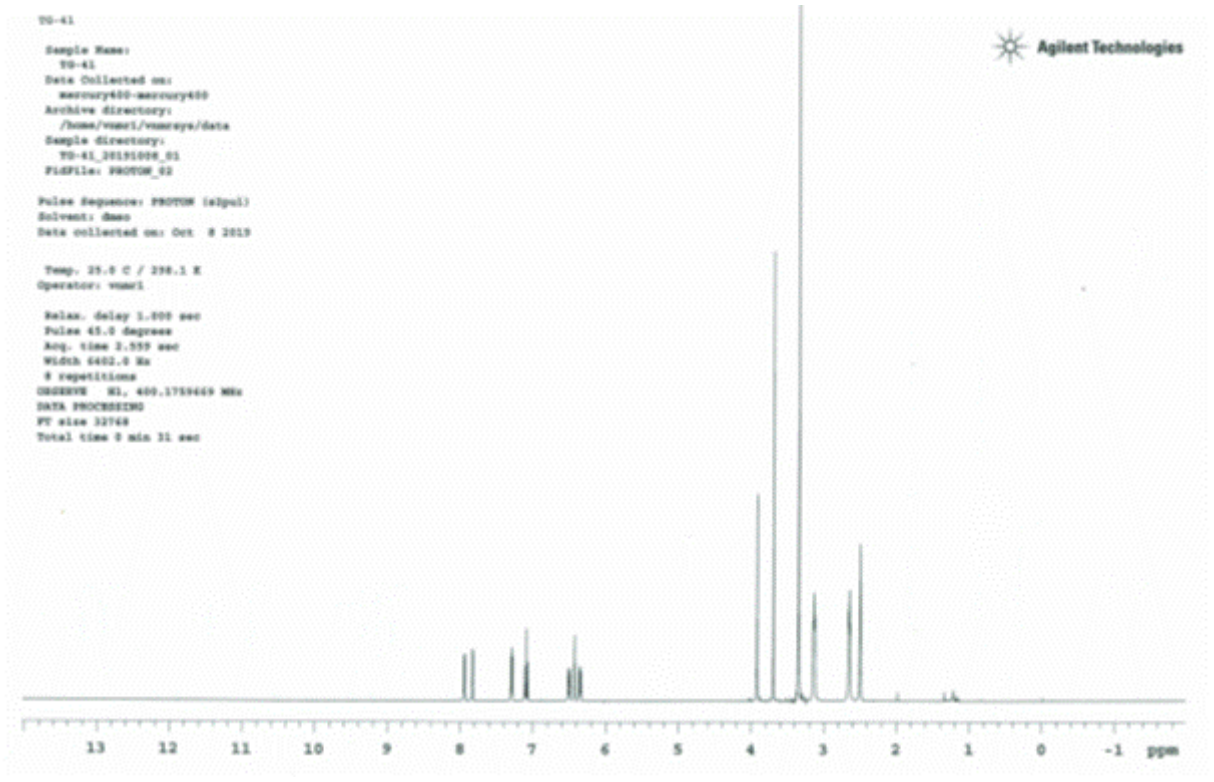

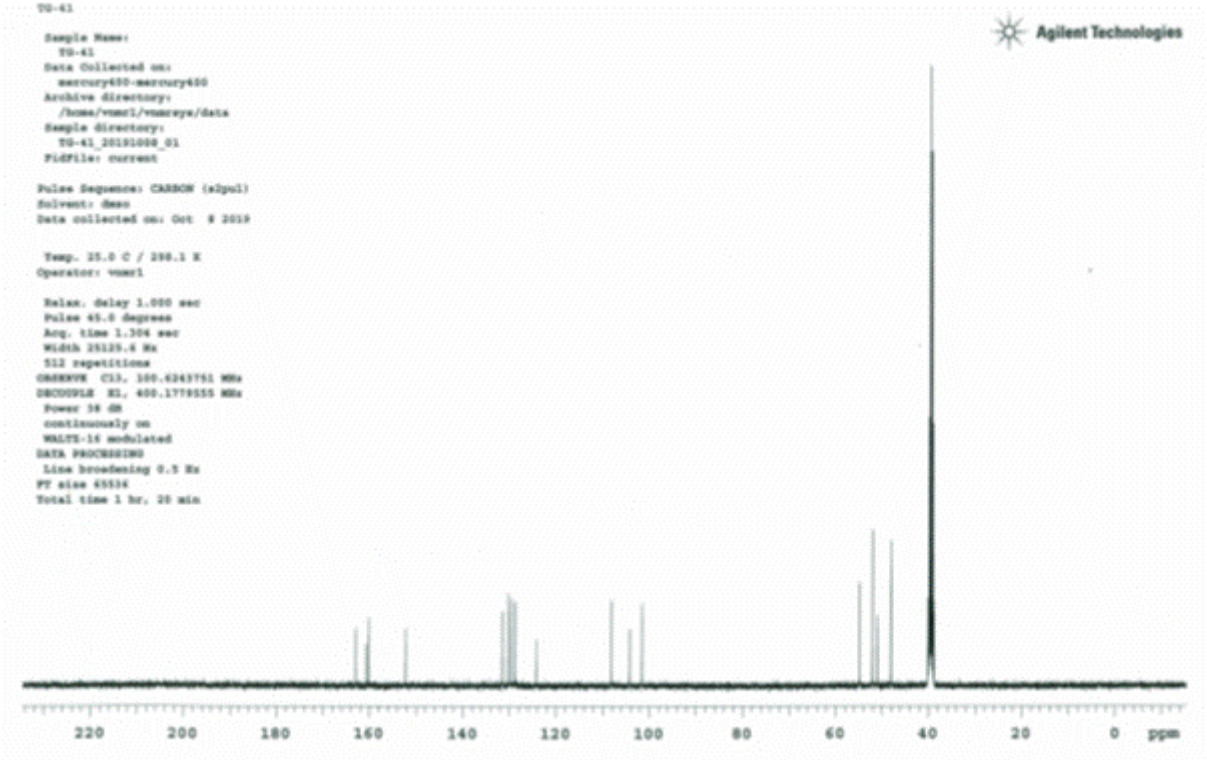
TG-41
Sample Name:
TG-41
Data Collected on:
mercury400-mercury400
Archive directory:
/home/vnmrl/vnmrsys/data
Sample directory:
TG-41_20191008_01
FidFile: current
Pulse Sequence: CARBON (s2pul)
Solvent: dmso
Data collected on: Oct 8 2019
Temp. 25.0 C / 298.1 K
Operator: vnmrl
Relax. delay 1.000 sec
Pulse 45.0 degrees
Acq. time 1.304 sec
Width 25125.6 Hz
512 repetitions
OBSERVE C13, 100.6243751 MHz
DECOUPLE H1, 400.1779555 MHz
Power 38 dB
continuously on
WALTZ-16 modulated
DATA PROCESSING
Line broadening 0.5 Hz
FT size 65536
Total time 1 hr, 20 min
Agilent Technologies
220
200
180
160
140
120
100
80
60
40
20
0
ppm

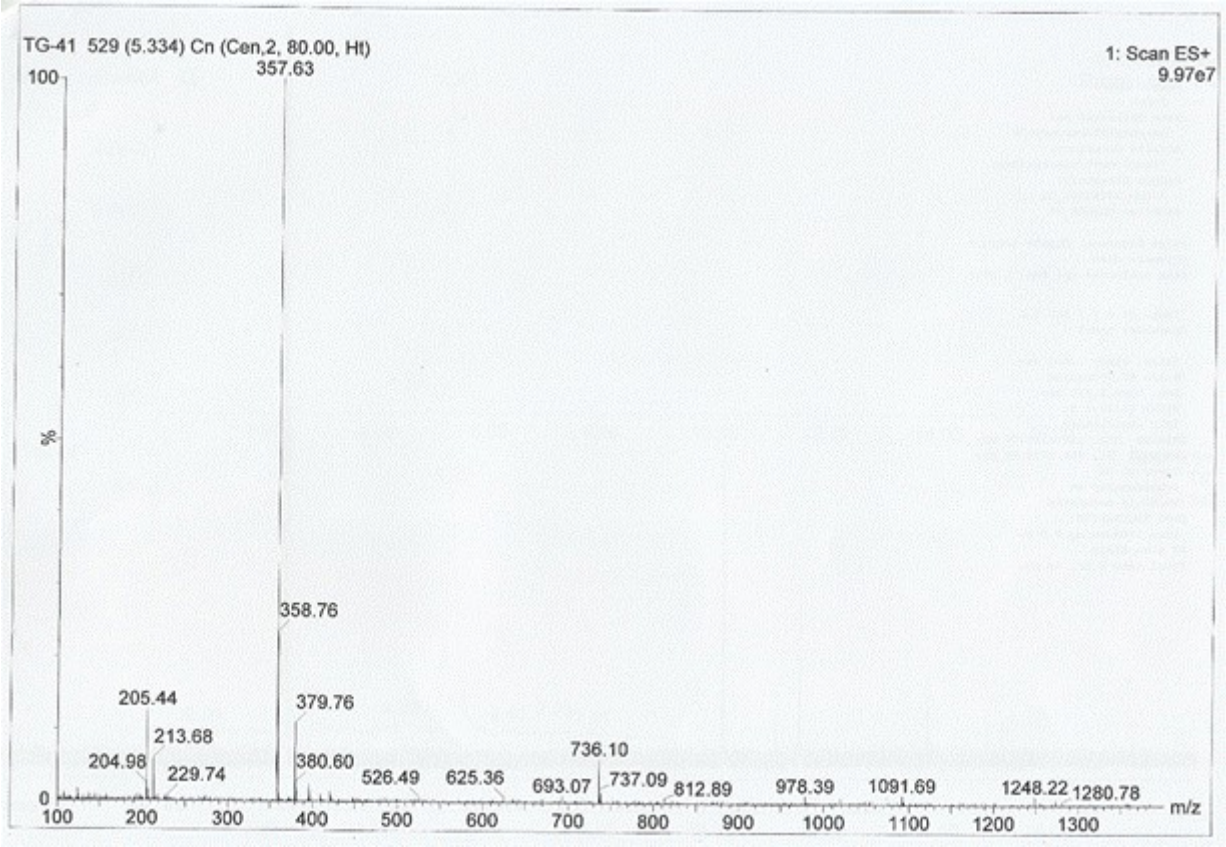
TG-41 529 (5.334) Cn (Cen,2, 80.00, Ht)
1: Scan ES+
9.97e7
100
%
0
357.63
358.76
205.44
213.68
204.98
229.74
379.76
380.60
526.49
625.36
693.07
736.10
737.09
812.89
978.39
1091.69
1248.22
1280.78
100
200
300
400
500
600
700
800
900
1000
1100
1200
1300
m/z

2-((4-(2-Fluorophenyl)piperazin-1-yl)methyl)-5-(thiophen-2-yl)-1,3,4-oxadiazole(8c)

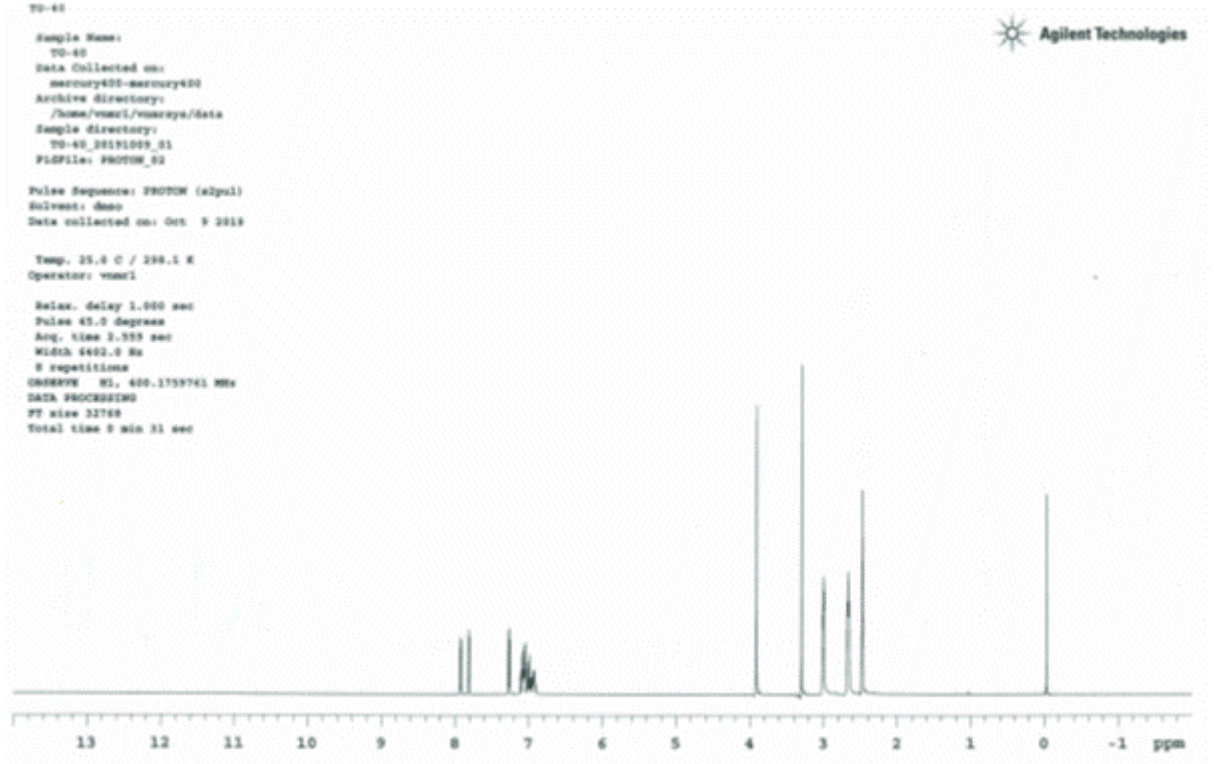

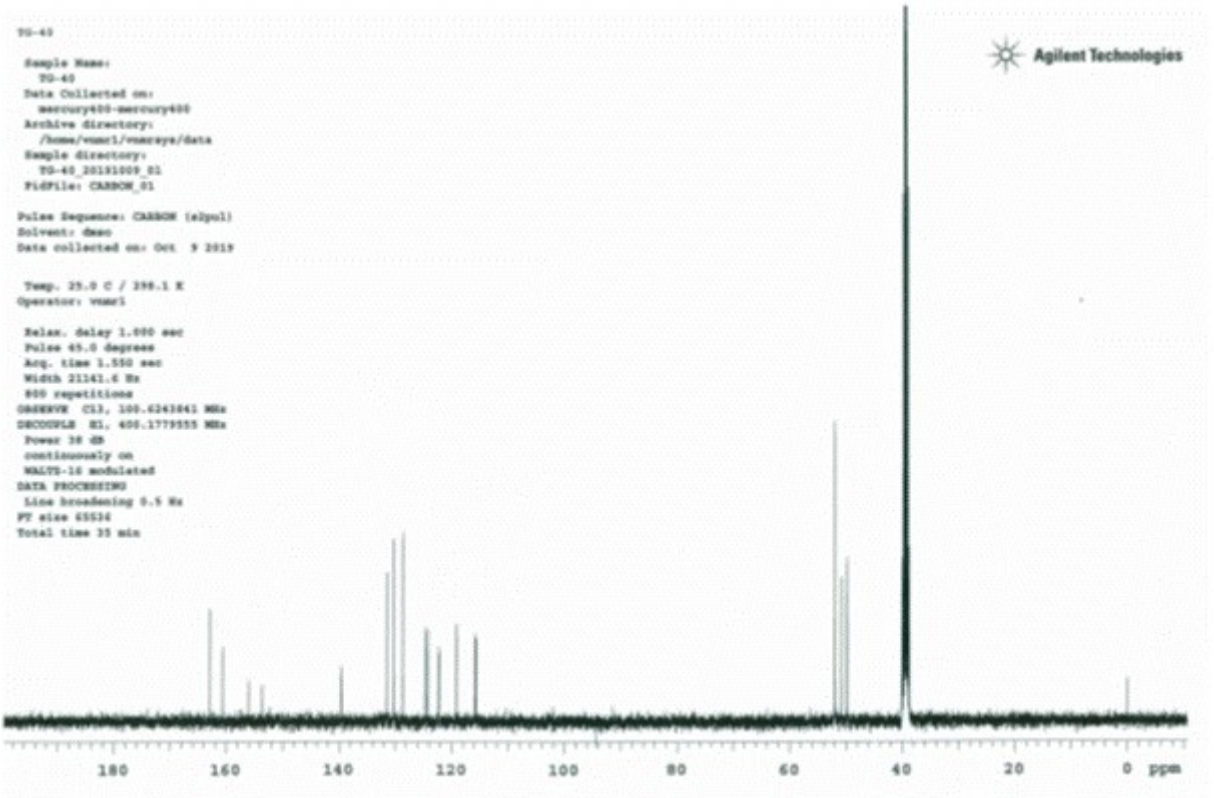

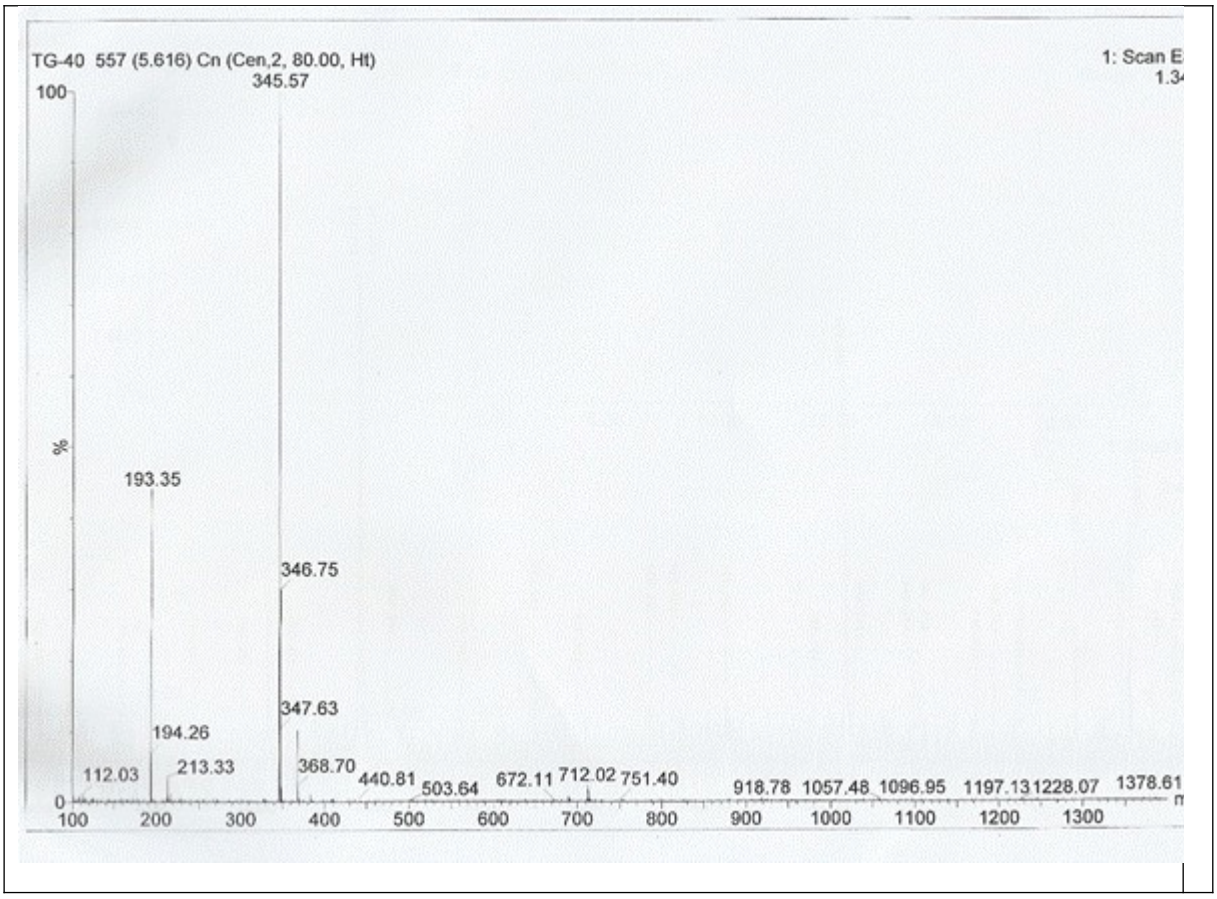

Docking results of compounds in active sites of EGFR and FAK kinases.

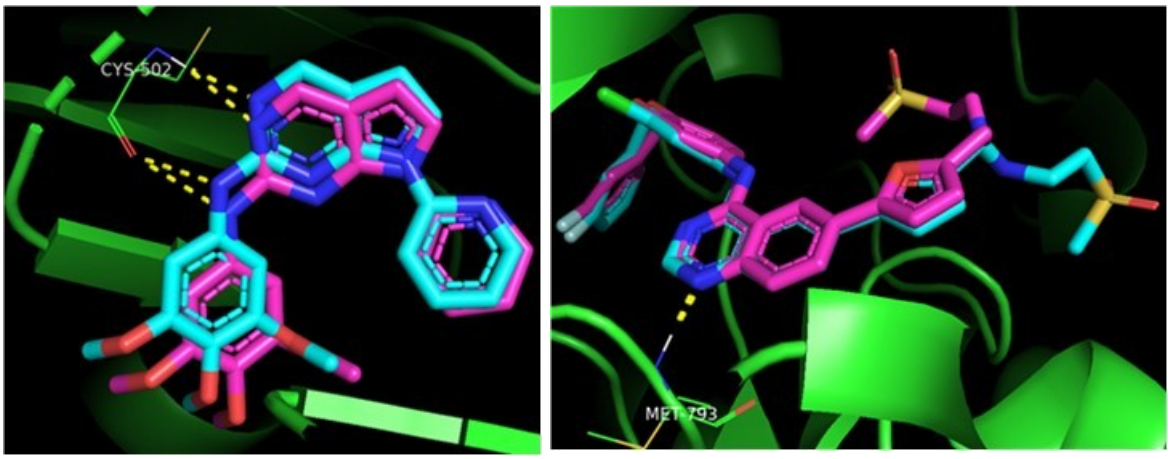

Figure S1. Superposition of native (blue) and docked ligand (magenta) of EGFR (1xkk, RMSD:1.42) (left). Superposition of native (blue) and docked ligand (magenta) of FAK (2etm, RMSD: 0.7) (right).

Table S1. The docking results of compounds with EGFR kinase

Compound	ΔGb[a] (kcal/mol)	Hydrogen bonds between atoms of compounds and amino acids	
		Atom of compound	**Amino acid**
4a	-9.0	-	-
4b	-9.4	O of oxadiazole	NH of Lys745
4c	-9.4	-	-
8a	-7.2	-	-
8b	-7.9	-	-
8c	-9.0	-	-
Native ligand		N-1 of quinazoline ring N-3 of quinazoline ring	NH of Met793 Thr854
Docked ligand	-11.2 RMSD[b]: 1.42	N-1 of quinazoline ring	NH of Met793

[a]Binding free energy, [b]root-mean-square deviation. –No interaction.

Table S2. The docking results of compounds with FAK kinase

Compound	ΔGb[a] (kcal/mol)	Hydrogen bonds between atoms of compounds and amino acids	
		Atom of compound	**Amino acid**
4a	-6.9	-	-
4b	-8.0	N3 of Oxadiazole	NH of Arg550
4c	-8.2	N3 of Oxadiazole N4 of Oxadiazole	NH of Arg550 OH of Ser568
8a	-6.1	N3 of Oxadiazole	NH of Gln432
8b	-7.6	N3 of Oxadiazole	NH of Gln432
8c	-7.6	N3 of Oxadiazole	NH of Gln432
Native ligand		N-3 of pyrimidine ring Exocyclic N	NH of Cys502 CO of Cys502
Docked ligand	-8.7 RMSD:0.7	N-3 of pyrimidine ring Exocyclic N	NH of Cys502 CO of Cys502

[a]Binding free energy, [b]root-mean-square deviation. –No interaction.